Scientific Examination of the Sculptural Polychromy of Cave 6 at Yungang

Francesca Piqué

The principal objective of the research described here[1] was to determine the nature and condition of the original and added materials of the paint layers and renders in Cave 6 at the Yungang grottoes. This study forms part of an overall program of investigation of the site by the Getty Conservation Institute and the State Bureau of Cultural Relics, who are collaborating on long-term conservation projects at Yungang and Dunhuang (Agnew and Huang herein).

The Yungang grottoes are Buddhist cave temples located in northern China, in Shanxi Province, near the Great Wall and the Mongolian border, though not specifically on the Silk Road.[2] Construction began at Yungang in 460 C.E., following the establishment of the capital of the Northern Wei emperor at Pingchang (modern Datong), about 15 km to the east. The caves were excavated in the south face of a sandstone cliff 800 m in length and 30–60 m in height (Fig. 1). There are fifty-three major caves, numbered from east to west, as well as fifty-one thousand niches and eleven hundred other smaller caves also excavated in the cliff stretch. The ruins of a fort, built in the Ming dynasty, are still present on top of the cliff. The work at Yungang lasted until the capital was moved south to Luoyang in 494 (Knauer 1983:29–33; Destenay 1986:877). One of the

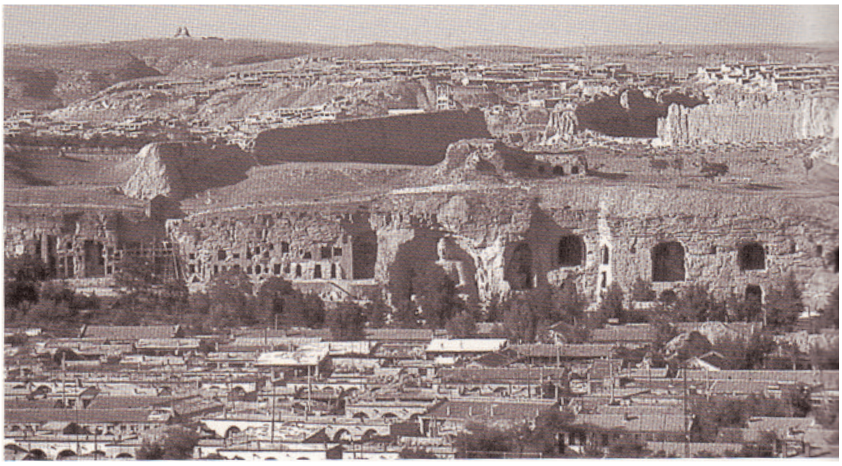

Figure 1
Yungang grottoes, general view of the western part of the south face of the cliff.

causes of the extreme deterioration of the cliff face is the erosion produced by the rainwater that runs down the inclined edge of the cliff top and washes off any loose material or particles of stone.

The concept of excavating cave temples from cliffs originated in India and spread from there to Afghanistan, Central Asia, and China. The first major Chinese Buddhist temple was built in the fourth century at Dunhuang (Falco Howard 1983:8). After the Northern Wei conquered the Gansu region in 439 C.E., thirty thousand families and three thousand monks were moved from Liangzhou-Wuwei, near Dunhuang, to the dynasty's new capital at Pingchang. This is of great importance because both the Buddhist doctrine and (most interesting for this research) the technique of excavating cave temples moved with these people from the west to the east. It is very likely that some of the same people who worked at Dunhuang were also involved in the early construction at Yungang. Indeed, the monk Tan-yao, who began and directed the excavation and carving work, came from Liangzhou-Wuwei in Gansu Province (Knauer 1983:33; Destenay 1986:877; Juliano 1984:81; Sickman and Soper 1956:90).

Cave 6 was built between 465 and 494 C.E. by Emperor Xiao Wen in memory of his mother and is one of the richest of the sites (Yungang Institute 1977:8; Destenay 1986:885). The cave is square in plan, with an almost square tower, or stupa pillar, at its center that rises to the ceiling. The entire interior surface of the cave is carved and painted; given the three-dimensional surface of the sculpture, the estimated surface area is approximately 1,000 m^2. Within this large area vast differences exist, in terms of condition, number of apparent repainting schemes, and materials used (Fig. 2). The upper and lower stories of the perimeter walls are each divided into three niches. Those of the upper stories house standing

Figure 2
Cave 6 interior, view of the southeastern corner of the upper story, showing painted walls, niches, and Buddhist sculptures. Here the carving is particularly well preserved. Thick deposits of dust are noticeable, particularly on the shoulder of the standing Buddha and the cornice that separates the lower from the upper story.

Buddhas surrounded by bodhisattvas, monks, and celestial flying figures. During sample collection, it was evident that there were at least three repainting phases, that the polychromy was brittle, and that it tended to fracture between paint layers and to separate from the support. Later analysis showed that there were many repainting phases (up to twelve), each composed of at least two layers. For these reasons, the identification of the original painting scheme and subsequent repainting phases was a difficult task. It was done by correlating the historical information and observation on-site with the stratigraphic evidence from the samples and the analytical results.

The history of the condition of Cave 6 is largely reflective of the various events that occurred at Yungang over the centuries, summarized in Table 1.[3] While much more information is available for recent events than for earlier ones, it is possible to relate restoration of the site with the destruction and rebuilding episodes usually associated with power struggles and dynastic wars. However, dates for restoration and repainting in a specific cave are seldom recorded, and therefore the association of a historical event with a particular repainting phase in Cave 6 has been made here only as a hypothesis.

The original materials of the polychrome sculpture were studied with optical and electron microscopy, microchemical tests, infrared microspectroscopy, X-ray diffraction (XRD), and energy-dispersive X-ray microanalysis (EDX). Pro forma examination and sampling were used to follow a coherent method of examination on-site and to collect all information on the samples. Each sample and sample location was also graphically and photographically documented.

Original Scheme

The primary purpose of the research was to determine the nature of the original scheme of polychromy, which was found to be characterized by a single, clay-based preparation layer and a single paint layer (Fig. 3). The preparation layer provides a smooth, compact surface as well as a background color for the paint layer. EDX analysis of the preparation showed the presence of large amounts of silica and aluminum and a small amount of potassium. The white material, visible as a large lump just under the paint layer, was identified by XRD as anglesite ($PbSO_4$) (JCPDS file 5-0577).

Figure 3
Example of cross section of original scheme. Cross section (×450) of a sample taken from the stupa pillar, south face, lower story, left arm of the fourth figure from the east. Starting from the upper part, the cross section shows a yellow-earth paint layer over a white, single-layer, clay-based preparation (original scheme).

Six pigments were identified in the original scheme. The resulting palette included a deep blue (natural ultramarine), a pale yellow (yellow earth), and several reds (vermilion, red lead, and red earth). It is surprising, particularly in comparison with a comprehensive compilation on contemporary paintings in Central Asia (Piqué 1992), that there is apparently no green pigment used in the original scheme. It is possible that green does occur but was not sampled during the present study, and this should be borne in mind in any future studies of this cave.

The yellow is an earth applied thinly over a white preparation (Fig. 3). The red pigments predominate in variety and use. Vermilion, red lead, and red earth were identified; all are common pigments used in Chinese polychromy. Vermilion and red lead were always applied over a red preparation. Red lead was found in all cases to have converted to plattnerite (PbO_2) (Fig. 4).[4] Plattnerite is the oxidation product of lead-containing pigments and occurs frequently in both Asian and Western paintings. Although the conversion process of lead white—$2PbCO_3 \cdot Pb(OH)_2$—has been well studied, that involving red lead (Pb_3O_4) has not been considered in detail. The oxidation of white lead to plattnerite (Pb^{2+} to Pb^{4+}) occurs by the following equation:

$$2PbCO_3 \cdot Pb(OH)_2 + 6OH^- = 3PbO_2 + 2CO_2 + 4H_2O + 6e^-$$

It is generally assumed that red lead conversion to plattnerite occurs by a similar oxidation process. However, experiments carried out at Dunhuang indicate that an intermediate step occurs, involving the formation of lead white (Li 1990:64–66). This seems to indicate that the conversion process is more complex (involving an initial alteration to lead carbonate) than has been previously considered for the conversion of lead white, formerly presumed to be analogous.[5]

Lead sulfate was identified by XRD in some of the white preparation layers of the original painting scheme (Fig. 3). In white preparation layers not from the original scheme, the high content of lead and sulfur shown by EDX analysis and examination by optical microscopy again suggested the possible presence of lead sulfate. It is notable that in two of

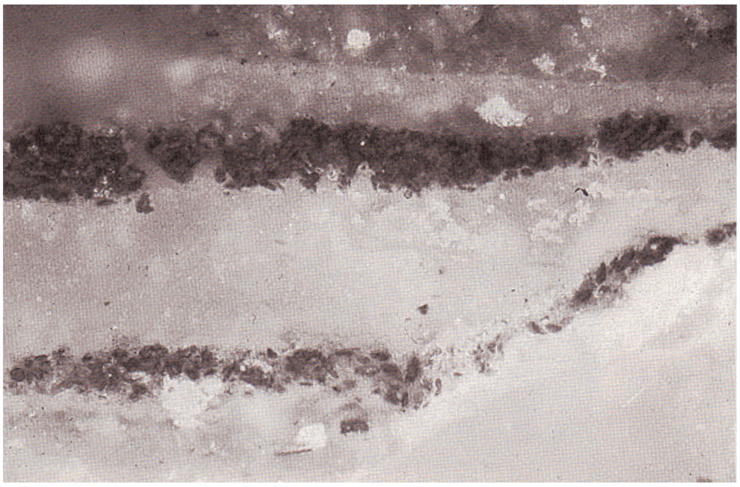

Figure 4

Cross section (×570) of original, first, and later schemes from a sample taken from the stupa pillar, east face, upper story, from the tunic of the central standing Buddha. Starting from the lower part, the cross section shows the white support, the red clay-based preparation layer, and red lead (completely converted to plattnerite) from the original painting scheme. From the first repainting scheme, a white single-layer preparation, composed of clay and gypsum, and darkened red lead are visible. From the repainting phase, a white clay-based preparation layer and a red paint layer, composed of red earth mixed with clay and gypsum, are visible.

these samples the lead-containing mixture had partially darkened. The dark material is very likely to be plattnerite because of the optical and elemental similarities with plattnerite as identified by XRD. Analysis by EDX of both darkened and unaltered particles shows a high content of lead and sulfur, but the lead:sulfur ratio is greater in the darkened particles, consistent with the formation of PbO_2 to the detriment of $PbSO_4$.

In the original scheme, the blue is a dark, natural ultramarine of high quality and large particle size, thickly applied. The sample shown in Figure 5 was collected in an area where much of the sculptural polychromy has deteriorated and the paint layer is almost completely lost in places. In this zone, traces of green thought to be part of the original scheme were identified and sampled. Subsequent examination of the cross section revealed the presence of this original paint layer composed of natural ultramarine below the green. The use of natural ultramarine at this early date is interesting; the mineral has been ascribed to various sources in Persia, China, and Tibet. The best quality lapis lazuli comes from Badakhshan in northeastern Afghanistan. Gettens identified ultramarine in fifth-century wall paintings from Kizil in Chinese Turkestan (Gettens 1938b:287–88). However, Kizil is located only 700 km from Badakhshan, and lapis lazuli would therefore have been much more easily available there than at Yungang, several thousand kilometers away.

First Repainting Scheme

A possible date for the first repainting scheme is 640 C.E.; at that time, during the early Tang dynasty, Yungang was incorporated in the prefecture of Yuncheng, and work was resumed at the Buddhist site (Table 1). Contemporary historical records report that the monk Yen was charged specifically with repairing the Northern Wei sculptures. Although this evidence is not conclusive, this is the first likely occasion for the repainting of Cave 6, some 150 years after its construction.

The first repainting scheme was found to be composed of only two colors: green, mainly composed of atacamite with some malachite and green earth; and red, from red lead converted to plattnerite (as in the original scheme). It seems odd that the palette would be so restricted; although this may be a function of the sampling, it may suggest that the

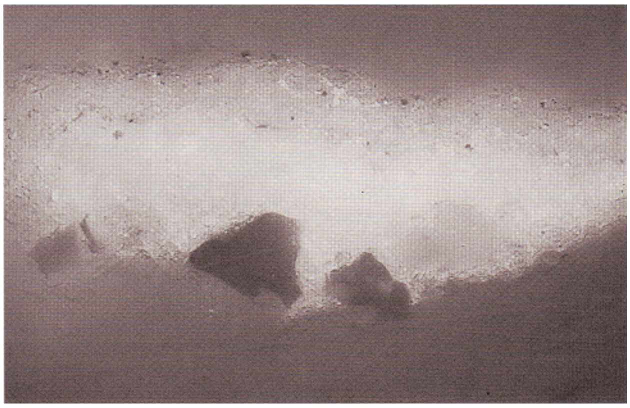

Figure 5
In this cross section (×490), starting from the lower part, the following stratigraphy can be seen: natural ultramarine (original scheme); clay and lead white and/or sulfate preparation, covered by a clay-based preparation (first repainting scheme—the green paint layer is not clearly visible).

first repainting scheme was carried out selectively within the cave.

Atacamite, one of three isomorphs (with paratacamite and botallackite) with the formula $Cu_2Cl(OH)_3$, occasionally mixed with some malachite and possibly green earth, was identified by XRD in six of the eight samples of the first repainting scheme. The optical characteristics of atacamite found in Cave 6—transparent green, globular rosettes with undular extinction, the occasional presence of a central dark core, and high relief (Fig. 6)—differ considerably from those of the natural mineral and may indicate a synthetic origin (Naumova, Pisareva, and Nechiporenko 1990:84). This type of mineral green pigment is commonly found at Dunhuang in wall paintings of almost all dynasties, including the Northern Wei (Xu et al. 1989; Moffatt et al. 1988:9).

Later Repainting Phases

As mentioned earlier, the substantial historical evidence indicating refurbishment, redecoration, and repainting at Yungang cannot be directly correlated with the scientific evidence of the stratigraphy. There are, however, several significant events that may have occasioned repainting in Cave 6, indicated in the chronology provided in Table 1. The general problems encountered in determining early painting schemes—including discontinuity due to partial repainting and/or partial loss—are compounded when trying to accurately identify successive repainting schemes. It was decided, therefore, to generally and collectively characterize stratigraphies not attributable to either the original or the first repainting scheme.

The technique of the various repainting phases that took place later does not differ significantly from that of the two earliest schemes. Dependence on the use of a ground and the tendency to apply paint in a single layer persist. The palette of the later phases—consisting of red, green, blue, yellow, black, and gold—is more extensive than that of the original and first repainting schemes. Three types of blue pigment are present: azurite, synthetic ultramarine, and an early type of Prussian blue. The range of yellows was expanded to include orpiment and massicot. Carbon black is also commonly found. An interesting addition is that of gold leaf, which was probably used to imitate gilded bronze sculpture. It was used on flesh areas, and remnants of gilding can be found on all of the figures. In one sample in which gold is used for flesh tone, there are four gold

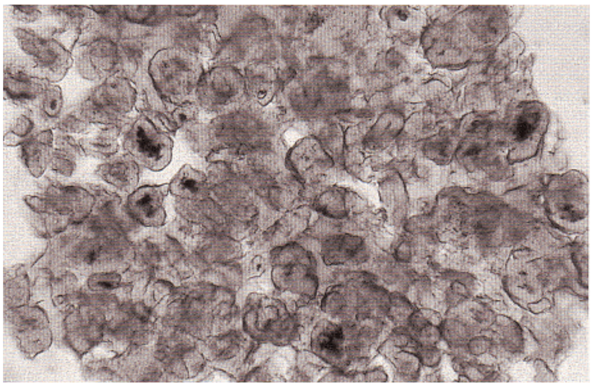

Figure 6
Photomicrograph (×450) in transmitted light of the green pigment found to be mainly composed of atacamite (by XRD, JCPDS file 25–269).

Table 1 Chronology, indicating possible repainting schemes

Date	Cave 6	Site	Historical events	Source
221 B.C.E.			First unification of China under Ch'in-shihuang-ti, who burned Confucian books	Knauer 1983:28
207 B.C.E.–220 C.E.		The site was important for its strategic position and was called Pingchang	Han Dynasty: resurgent Confucianism, funerary art	Knauer 1983:28
111 B.C.E.			Dunhuang established as a prefecture	Dunhuang Institute of Cultural Relics 1983:251
First century C.E.			Buddhism reached China along Silk Road from India	Knauer 1983:28
Early fourth century C.E.			Toba tartars (future Northern Wei dynasty) occupied territories north of Yellow River	Knauer 1983:28
386–535			Northern Wei dynasty: Buddhism became imperial religion	Falco Howard 1983:7
398		Northern Wei capital established at Pingchang (Datong)	Reign of emperor Toba Kuei	Knauer 1983:29 Destenay 1986:877
439		3,000 captive monks and 30,000 families moved from Liangzhou-Wuwei in Gansu Province (near Dunhuang) to Datong	Emperor Tai Wu conquers Gansu Province (including Dunhuang)	Knauer 1983:33 Destenay 1986:877 Juliano 1984:81 Sickman and Soper 1956:90
446–452			Buddhism persecution: disruption of temples and monastery	Knauer 1983:29 Sickman and Soper 1956:87
452–454			Restoration of Buddhism	Knauer 1983:30 Sickman and Soper 1956:87
455		Five Indian monks, sculptors, and painters arrived in Datong		Destenay 1986:878
460–485		Beginning of work at Yungang, directed by the monk Tan-yao (who was from Liangzhou)		Destenay 1986:878 Sickman and Soper 1956:87 Juliano 1984:82
465–494	Construction by Emperor Xiao Wen (471–500) in memory of his mother			Yungang Institute 1977:8 Destenay 1986:885
494	Completed when the capital was moved to Luoyang	End of most active work but some continues; site remains an important Buddhist center	Capital moved from Datong to Luoyang (south)	Yungang Institute 1977:10 Sickman and Soper 1956:87 Knauer 1983:32–33
523		Rebels controlled Pingchang for 7 years; beginning of decline of Yungang as Buddhist center		Yungang Institute 1977:13
640	*Possible repainting phase*	Construction work resumed: a monk, Yen, in charge of repairing the Northern Wei images	Yungang incorporated into the prefecture of Yuncheng (early Tang dynasty, 618–906)	Yungang Institute 1977:13

Table 1 continued

Date	Cave 6	Site	Historical events	Source
1049–1059	Site of the Tienkung Monastery *Possible repainting phase and first use of mud plaster repair*	Construction of 10 wooden monasteries and other structures in front of the caves. Repair of 1,876 large and small Buddhist images; some images added	1044: Datong established as one of the five capitals; revival of Buddhism	Yungang Institute 1977:13 Knauer 1983:33 Mizuno and Nagahiro 1955: vol. 2, 56–57 Juliano 1984:85
1122		Attack by Jin army; all 10 monasteries were burnt	Liao-Jin dynasties war episodes	Yungang Institute 1977:8 Juliano 1984:85
1143–1146	*Possible repainting phase*	Cave temples repaired by monk Ping Huei	Jin dynasty (1125–1234)	Yungang Institute 1977:14
1305		Strong earthquake destroyed 4,800 houses; 1,400 people killed	Yuan dynasty (1271–1368)	Xie 1992
1548–1558	*Possible repainting phase*	Caves were repaired and restored	Ming dynasty (1368–1644)	Yungang Institute 1977:14
1644		All buildings destroyed. Any wooden structure visible now is post-1644	Qing dynasty (1644–1911), occupation of Datong	Yungang Institute 1977:14 Juliano 1984:85
1651	Wooden monastery built in front of Caves 5 and 6 *Possible repainting scheme*	Under emperor Shun Zhi, work carried out		Yungang Institute 1977:14 Knauer 1983:33 Tablet in Cave 5 Juliano 1984:50
1696–1698	*Possible repainting scheme*	Emperor Kang Xi visited the site. The monastery was reconstructed		Tablet in Cave 5 Yungang Institute 1977:14 Destenay 1986:883
1769	*Possible repainting scheme*	The monasteries repaired: gilding of flesh areas on figures	Reign of emperor Qian Long (1736–1796)	Yungang Institute 1977:14
1861		Construction of buildings in front of the caves		Tablet in Cave 5
1876		Small house built in front of caves: decoration of Buddhas		Tablet in Cave 6
1892	*Possible repainting scheme*	Visit of emperor: general cleaning and repainting of the caves, Caves 9–13 gilded and decorated	Reign of emperor Guang Xu (1875–1909)	Tablets in Cave 9 (set up in 1920)
1938–1945	Heavy repainting on stupa and soffit recorded	Mizuno and Nagahiro worked at Yungang		Knauer 1983:27 Mizuno and Nagahiro 1955
1940		Precinct built around the site		Mizuno and Nagahiro 1955: vol. 2, 56
1949		Flood; after liberation, works were carried out at the site		Knauer 1983:33 Huang 1992 Tablet in Cave 7
1955	Wooden temple in front of Caves 5, 6, and 7 restored	Foundation of the Institute for the Preservation of the Yungang Caves. Entire site cleared		Destenay 1986:885
1988		Beginning of GCI project		
1992		Archaeological excavation in front of cave 20: gilded fragments found		

layers but no evidence of any other type of colored paint layer, indicating that gold was used during the last four surviving repainting phases.

Comparison with Previous Scientific Examination of Chinese Polychromy

Technical literature provides substantial data for comparison with the results from Cave 6 at Yungang. Relevant technical literature, selected on the basis of date, site, and type of object, is summarized in Table 2. Articles are arranged by the date of publication, and the analytical methods used for examination are given. It is evident from this table that there is a time gap between the early work of Gettens, carried out with polarized-light microscopy (PLM), microchemical tests (MCT), and recent instrumental analysis beginning in the 1980s. Moreover, there is no scientific examination on sculptural polychromy of the fifth century, which would be directly comparable to that of Yungang. Substantial data remains,

Table 2 Summary of relevant technical literature on Chinese and Central Asian polychromy

Date of publication	Author	Analytical methods	Object date	Object type	Site or culture[1]
1921	Church	PLM, MCT	not given	wall paintings	Dunhuang and others
1935[2]	Gettens	PLM, MCT	C15	wall paintings	Dunhuang
1936[2]	Gettens	PLM, MCT	Tang dynasty (618–907) and earlier	wall paintings and sculptures	Dunhuang
1938c	Gettens	PLM, MCT	Ming dynasty (1368–1644)	wall paintings	Hua Yen Ssu Shanxi
1938a	Gettens	PLM, MCT	late C6	wall paintings	Bamian, Afghanistan
1938b	Gettens	PLM, MCT	C5–9	wall paintings	Kizil, Chinese Turkestan
1982, 1983	Moffatt and Adair	XRD, FTIR, SEM-EDX	1279–1368 Yuan dynasty	wall paintings	Shanxi, near Yung-Lo
1992	West FitzHugh and Zycherman	PLM, XRD, SEM-EDX	204 B.C.E.–221 C.E. Han dynasty	blue pigment	Chinese
1985	Larson and Kerr	PLM, MCT, XRF, GC-MS	1115–1234 Jin dynasty	sculpture	Putuo Shan Zhejian, East China
1987	Duang et al.	XRD, EPMA	not given	wall paintings	North China
1988	Larson	PLM, MCT, XRF GC-MS	Tang and Jin dynasties and C8–13	sculptures	Chinese
1988	Moffatt et al.	XRD, FT-IR, SEM-EDX	not given	wall paintings	Dunhuang
1989	Dunhuang Academy	XRD	618–907 Tang 960–1271 Song	wall paintings Caves 35 and 232	Dunhuang
1989	Xu et al.	XRD, XRF	from 304–C19 Sixteen to Qing dynasty	wall paintings	Dunhuang
1992	West FitzHugh and Zycherman	PLM, XRD, SEM-EDX	204 B.C.E.–221 C.E. Han dynasty	purple pigment	Chinese

[1] Where the object is unprovenanced, the cultural designation is given instead.

[2] Unpublished reports.

PLM = polarized-light microscopy; MCT = microchemical test; XRD = X-ray diffraction; FT-IR = Fourier-transform infrared spectroscopy; SEM-EDX = scanning electron microscopy-energy dispersive X-ray spectrometry; XRF = X-ray fluorescence; GC-MS = gas chromatography-mass spectrometry.

nevertheless, and this has been extracted and organized by pigment in Piqué 1992, tables 6.2–6.17. Most past analytical work has been undertaken on wall paintings, particularly at Dunhuang; but data on sculptural polychromy is also available and of great interest. The most striking conclusion obtained from this tabulation is that the techniques of the polychromy do not vary significantly in relation to the type of support—whether stone, mud, or wood. In fact, the support does not correlate significantly with the object type; both wall paintings and sculptures may be on either mud or stone. The common basic technique, consistent with the findings at Yungang, is the use of a clay-based ground under the paint layers.

Areas for Future Study

This study of the polychromy of Cave 6 at Yungang has provided significant information on the original and subsequent painting schemes of the sculptured decoration. However, due to the constraints on in situ examination, sampling, and analysis, a number of issues were not fully resolved and require further research. Moreover, consideration of the historical and technological importance of the painted decoration of Cave 6 within the wider context of Central Asian and Chinese polychromy was severely restricted by the relative paucity of similar research and by the lack of access to much of the primary Chinese literature on paintings. The principal issues requiring further research are the alteration of lead-containing pigments, the synthesis and use of atacamite, the nature and use of clays, the nature and use of organic binders, and the absence of green in the palette of the original scheme.

A conspicuous finding was the deterioration of lead. All the samples of red lead from the original scheme were found to be entirely altered to plattnerite, whereas in the later layers, red lead is found unaltered, partially altered, and fully altered. Additionally, both lead white and lead sulfate were found to be partially converted to plattnerite. Clearly, the mechanism of and conditions for the conversion of these lead-containing pigments to lead dioxide is of considerable interest, particularly with regard to implications they may hold for conservation.

Another area that may prove fruitful for further investigation is the synthesis and use of atacamite. The present study has not only demonstrated its extensive use in Cave 6 over a long period of time but also suggests that other tentatively or inconclusively identified greens in Chinese polychromy may be atacamite. Copper-chloride greens are increasingly being identified in Western medieval paintings, though in many cases they may be the alteration products of copper-carbonate greens. Their apparently widespread use in Chinese paintings during the same period is significant, and further study would be of interest not only in the context of Chinese painting technology but also in regard to Western practice.

Some of the green particles that were found mixed with atacamite and malachite were tentatively identified as green earth, even though the elemental analysis of the green mixture showed that the main components were copper and chloride. Other green particles, however, did not show any characteristic features in transmitted-light examination. A recent study

Figure 7
Cave 6, stupa pillar, east face, lower story, lower part of third figure from west, enlarged detail showing traces of paint layer flaking from the stone support. Large amounts of dust are deposited at the feet of the figure and also behind the flakes of the paint.

(Martin and Eveno 1992:785) has shown that copper pigments often have heterogeneous composition, and that to fully understand the nature of such a mixture, both XRD and elemental analysis should be carried out on all types of particles present.

The use of clay seems to be the most characteristic feature of Central Asian and Chinese polychromy. The tentative hypothesis that fired clay was ground and used for at least some of the preparation layers of Cave 6 certainly merits further investigation. It would, therefore, be highly desirable to undertake an exhaustive study of clays: their components and their physical and aesthetic functions. This would require in-depth analysis of clay types, their mineral inclusions, and the probable organic binders used, as well as their correlation with paint layers to interpret their function within the overall stratigraphy.

It has not been possible during this research to undertake analysis of the organic binding media used. Clearly, this would be highly desirable, particularly with regard to the implications for future conservation. However, present insights into the various painting phases revealed by the components and layer structure of the polychromy are a necessary preliminary step for any such study.

While the general conclusions regarding the relationship of the polychromy of Cave 6 to the wider context of Central Asian and Chinese paintings seem to be valid, the constraints on making such conclusions are considerable, as there is little comparable technical analysis. The important work now being carried out by the Dunhuang Academy is doing much to elucidate the technologies of the paintings of various periods in Dunhuang. However, Yungang is almost 2,000 km east of Dunhuang, thus separated from direct influences carried along the Silk Road; the extent to which the technology of its polychromy reflects or adapts early Chinese (as opposed to Central Asian) techniques is simply not known. Apart from the technical examination of earlier Chinese polychromy (particularly of the Han and Sixteen dynasties), another obvious source of the context of the Yungang paintings would be primary sources and documents. These are considerable, and to evaluate them would clearly require expert knowledge of both their language and history.

As indicated, some of the further research proposed here would have implications for the conservation of polychromy, particularly analysis of the media and investigation of the causes of lead alteration. However, an additional factor is the serious threat posed by the development of the coal industry at adjacent Datong, one of China's largest coal producers, whereby a fine black dust is continuously and heavily deposited on the sculptures (Figs. 2, 7). Apart from the physical and chemical interaction this may cause (Christoforou, Salmon, and Cass herein), an immediate and serious danger is the dusting regularly undertaken to remove this deposit. Considering the extremely fragile condition of the surviving polychromy—often tenuous adhesion between various layers of paint, and the widespread flaking evident (Fig. 7)—dusting is likely to be one of the major factors presently causing the loss of the paint layers. It is therefore necessary, first, to attempt to reduce the amount of dust deposited and, second, to improve the methods of dusting. Obviously, the problem of flaking that is common to the entire site should also be resolved; however, this would require an extensive investigation both of the causes and of suitable conservation methods and materials.

Acknowledgments

The author wishes to thank Neville Agnew, associate director, Programs, and Dusan Stulik, then deputy director, Scientific Program, both at the Getty Conservation Institute; and the Courtauld Institute of Art, especially Sharon Cather, for their generous support and guidance. The author is also grateful for the support of Huang Kezhong, deputy director of the National Institute of Cultural Property in Beijing; and Fan Jinshi, deputy director of the Dunhuang Academy.

Notes

1 This research project was undertaken by the author in partial fulfillment of her M.S. degree in wall painting conservation at the Courtauld Institute of Art. The analytical work was carried out at the Getty Conservation Institute.

2 See map of Asia, pages xiv–xv.

3 Bibliographic citations for the information included in the chronology are given in Table 1 and are not repeated here.

4 Plattnerite (PbO_2) may occur as the oxidation product of either white or red lead (Giovannoni et al. 1990:21), but the original pigment cannot be determined analytically from the altered material. Consequently, determination of the original color is made on the basis of circumstantial evidence—particularly the presence of unconverted particles in the paint layer and the likely coloristic intent—as indicators of the original pigment. In this case, the strongest evidence indicating this is the use of a red preparation beneath all samples.

5 Considering that in the red lead (Pb_3O_4) the lead is not at a single state of oxidation but rather two lead atoms are found at the lower oxidation state (Pb^{2+}) and one at the higher oxidation state (Pb^{4+}), and lead white contains only Pb^{2+}, this type of process would be composed of a first reduction (of the one Pb^{4+} atom in red lead to Pb^{2+} in white lead) followed by an oxidation of Pb^{2+} to Pb^{4+} (oxidation state in plattnerite).

References

Church, A.

1921 Examination of certain specimens of mural paintings and plaster from Ak-terek, Karasai, Khadalik, Miran, Ming-oi and Tun-huang. In A. Stein, *Serindia*. Vol. 3, app. D: 1390–91. Oxford: Clarendon Press.

Destenay, Anne L.

1986 Yungang. In *China,* 876–91. Geneva: Nagel Publishers.

Duang Shuye, Jun-Ichi Miyata, Noriko Kumagai, and Ryuitiro Sugisita

1987 Analysis of pigments and plaster from wall paintings of Buddhist temples in northwest China. *Scientific Papers on Japanese Antiquities and Art Crafts* 32:13–20.

Dunhuang Academy

1989 An X-Ray Analysis Report on Inorganic Pigments of Caves 232 and 35 Murals in Mogao Grottoes. Report. Dunhuang Academy.

Dunhuang Institute of Cultural Relics

1983 *The Art Treasures of Dunhuang.* Hong Kong: Joint Publishing Company.

Falco Howard, A.

1983 *Chinese Buddhist sculpture from the Wei through the Tang dynasties.* Taipei: Chung-hua min kuo kuo li li shih po wu kuan.

Gettens, R. J.

1935 Preliminary Report on Chinese Pigments. Cambridge: Center for Conservation and Technical Studies, Harvard University Art Museum, Cambridge, Mass.

1936 The Pigments from Central Asian Paintings. Report. Center for Conservation and Technical Studies, Harvard University Art Museum, Cambridge, Mass.

1938a The materials in the wall paintings from Bamiyan, Afghanistan. *Technical Studies in the Field of Fine Arts* 6:186–93.

1938b The materials in the wall paintings from Kizil in Chinese Turkestan. *Technical Studies in the Field of Fine Arts* 6:281-94.

1938c Pigments in a wall painting from central China. *Technical Studies in the Field of Fine Arts* 7:99–105.

Giovannoni, Sabino, et al.

1990 Studies and developments concerning the problem of altered lead pigments in wall paintings. *Studies in Conservation* 35:21–25.

Huang Kezhong

1992 Conversation with author, Yungang grottoes, May.

Juliano, A. L.

1984 New discoveries at the Yungang caves. In *Chinese Traditional Architecture* (catalogue of exhibition at China Institute in America, China House Gallery, New York), ed. N. Shatzman Steinhardt et al., 79–89. New York: China Institute in America, China House Gallery.

Knauer, E. R.

1983 The fifth-century A.D. Buddhist cave temples at Yun-kang, North China. *Expedition* 25(4):27–47.

Larson, John H.

1988 The treatment and examination of Chinese sculpture at the Victoria and Albert Museum. In *The Conservation of Far Eastern Art: Preprints of the Contributions to the Kyoto Congress, 19-23 September 1988,* ed. J. S. Mills, P. Smith, and K. Yamasaki, 120–25. London: International Institute for the Conservation of Historic and Artistic Works (IIC).

Larson, John H., and R. Kerr

1985 *Guanyin: A Masterpiece Revealed.* London: Victoria and Albert Museum.

Li Zuixiong

1990 Research on the Discoloration of Red Pigments of the Dunhuang Wall Paintings. Thesis. Dunhuang Academy.

Martin, E., and M. Eveno

1992 Contribution to the study of old copper pigments in easel paintings. In *Third International Conference on Nondestructive Testing, Viterbo, 4–8 October 1992,* 781–91. Rome: Beta Gamma Editrice.

Mizuno, S., and T. Nagahiro

1952–56 *Yungang: The Buddhist Cave Temple of the Fifth Century A.D. in North China: Detailed Report of the Archaeological Survey Carried Out by the Mission of the Toho Bunka Kenky'sho, 1938–1945* (in Japanese). 16 vols. Kyoto: Jimbunkagaku Kenkyusho, Kyoto University.

Moffatt, E., and N. Adair

1982 Ars 1900, Ars project 13D, *The Lord of Southern Dipper.* Analytical report. Canadian Conservation Institute (CCI).

1983 Ars 2094: *The Lord of the Northern Dipper;* Ars 2095: *The Paradise of Maitreia.* Analytical report. CCI.

Moffatt, E., P. J. Sirois, G. S. Young, and I. U. M. Wainwright

1988 Contribution to the Analysis of Wall Painting Fragments and Related Materials from the Mogao Grottoes at Dunhuang, People's Republic of China. Report. CCI.

Naumova, M. M., S. A. Pisareva, and G. O. Nechiporenko

1990 Green copper pigments of old Russian frescoes. *Studies in Conservation* 35:81–8.

Piqué, Francesca

1992 Scientific Examination of the Sculptural Polychromy of Cave 6, Yungang. Master's thesis. Courtauld Institute of Art, University of London.

Sickman, L., and A. Soper

1956 *The Art and Architecture of China.* Baltimore: Penguin Books.

West FitzHugh, E., and L. A. Zycherman

1992 A purple barium copper silicate pigment from early China. *Studies in Conservation* 37(3):145–54.

Xie Tingfan

1992 Conversation with author, Yungang grottoes, May.

Xu Weiye, et al.

1989 An X-ray analysis report on inorganic pigments of wall paintings and painted sculpture in the Mogao grottoes (in Chinese). *Dunhuang Yanjiu* 1989:7–26.

Yungang Institute, Committee in Charge of the Cultural Relics and the Institute for the Preservation of the Yungang Caves of Shanxi Province

1977 *The Yungang Caves.* Beijing: Wenwu Chubanshe.

Pigment Analysis of Polychrome Statuary and Wall Paintings of the Tiantishan Grottoes

Zhou Guoxin, Zhang Jianquan, and Cheng Huaiwan

The Tiantishan grottoes are situated on the Huangyang River, about 60 km south of Wuwei (originally Liangzhou) and were excavated during the Northern Liang dynasty (397–439 C.E.). Carving and decoration of the grottoes continued throughout the Northern Wei, Tang, and Ming dynasties, leaving many precious cultural relics inside these grottos.

On the basis of the style, content, and inscriptions on the wall paintings and landforms, archaeologists believe that the Tiantishan grottoes may be the Liangzhou grottoes mentioned in historical documents, such as the *Fa Yuan Zhu Lin*. According to historical records, the Liangzhou grottoes were ranked with the Yungang and Longmen grottoes as the three major cave temple sites to have exerted profound influence on the development of Chinese painting and sculpture. If the Tiantishan and Liangzhou grottoes are actually one and the same, research and protection of this site becomes even more meaningful and important.

Because of the construction of the Huangyang River reservoir in 1960, the Gansu People's Government approved moving the wall paintings and polychrome statues of the grottoes, with the exception of seven cliff statues, to the Gansu Provincial Museum for preservation. In conjunction with the restoration and conservation of the Tiantishan relics, the authors collected and analyzed ninety-six samples from the Northern Liang, Northern Wei, Tang, and Ming dynasties and performed comprehensive analyses of their pigments.

Experimental Principles and Methods

X-ray diffraction analysis is capable of accurate and rapid analyses of pigments from polychrome statues and wall paintings. Only small quantities of sample are required, it is not necessary to chemically separate the samples, and the samples are not destroyed. The samples that have been analyzed can be stored in the form of index cards for future comparative use. X-ray fluorescence analysis is an important auxiliary technique to X-ray diffraction that can increase the reliability of the results of analysis (Xu, Zhou, and Li 1983).

Analytical Results

Detailed records were made of the sampling sites at the time of sampling. Results of the analyses are presented in Table 1. The pigments that were used over the course of the successive dynasties in the Tiantishan grottoes and the circumstances of their use can be ascertained from the table.

In the samples taken from the Northern Liang dynasty, gypsum and anhydrite were the major white pigments, cinnabar was the red pigment, and malachite was the green pigment. Lead hydroxychloride and lead sulfate were used in addition to gypsum and anhydrite for color blending.

In the Northern Wei samples, anhydrite and kaolin were the major white pigments; cinnabar and malachite were used; and azurite was the blue pigment with gypsum, anhydrite, and kaolin added for color blending.

In the Tang dynasty samples, the Tang polychrome sculpture had two layers. Gypsum and lead white were the major white pigments, cinnabar and minium were the red pigments, and azurite and malachite were also used. Gold powder and gold leaf were used for the gold color, and gypsum and lead white were used during the color blending process. For the outer layer, the major white pigments were lead white, lead sulfate, gypsum, and kaolin; the red pigments were cinnabar and minium; the blue pigment was azurite; the green pigments were malachite, basic copper chloride, and hydrated basic copper chloride; the brown pigments were lead dioxide (an oxidation product of minium); and the gold pigments were gold powder and gold foil. In addition to lead white, gypsum, lead sulfate, and kaolin, many other pigments, such as lead hydroxychloride, chalk, and a natural mineral—leadhillite, $PbSO_4 \cdot 2PbCO_3 \cdot Pb(OH)_2$—were added for color blending. The colors used were complex. The white pigment for the Tang wall paintings was gypsum, and the red pigment was hematite.

In the Ming dynasty wall paintings sampled, kaolin, gypsum, and lead sulfate were the major white pigments. The red pigments were cinnabar and minium; the green pigments were malachite, basic copper chloride, and hydrated basic copper chloride; the blue pigment was azurite; and the yellow pigment was orpiment. Soot was the black pigment used during all of the dynasties mentioned here.

Discussion

Calcium oxalates (calcium oxalate monohydrate and calcium oxalate dihydrate), which are compounds of organic origin, are commonly associated with plant fossils. Many samples examined in this study contained calcium oxalates. Similar results were also observed in the Maijishan grottoes of Gansu Province and the Yungang grottoes of Shanxi Province (Zhou 1991; X-ray Diffractometer Users' Association 1983). There are no specific reports as to whether calcium oxalates were used as pigments or whether they were formed later; further study will be required on this matter.

In the present work, the authors found that the colors of the pigments used in the Tiantishan grottoes were rich and vivid. Malachite, atacamite-type basic copper chloride, paratacamite basic copper chloride, and hydrated basic copper chloride were used as the green pigments.

Table 1 Pigment analysis results

Dynasty	Cave no.	Sample no.	Color	XRF	XRD	Pigment phases	Note
Northern Liang	4	01	Red		cinnabar, lead chloride, trace calcite, quartz	cinnabar	
Northern Liang	4	02	Black		quartz, mica	ink	
Northern Liang	4	03	Green	Cu, Pb	quartz, lead sulfate, malachite, gypsum	malachite	
Northern Liang	4	04	White		gypsum, trace anhydrite	gypsum, anhydrite	
Northern Wei	1	05	Green		malachite, trace gypsum, kaolin, quartz	malachite	
Northern Wei	1	06	Red		cinnabar, quartz, trace gypsum, kaolin	cinnabar	
Northern Wei	1	07	Blue-green		azurite, quartz, feldspar, calcite, anhydrite	azurite	
Northern Wei	1	08	Red		cinnabar, anhydrite, quartz	cinnabar	
Northern Wei	1	09	Black		anhydrite, trace quartz	ink	
Tang	2	10	Ground		quartz, kaolin, calcite, feldspar, mica		inner layer [a]
Tang	2	11	Ground		quartz, kaolin, feldspar, calcite		outer layer
Tang	2	12	White		gypsum, quartz, trace kaolin	gypsum	inner layer
Tang	2	13	Light green		gypsum, malachite, quartz, trace lead white	malachite	inner layer
Tang	2	14	Red		gypsum, minium	minium	inner layer
Tang	2	15	Green		malachite, trace quartz, mica	malachite	outer layer
Tang	2	16	Black		quartz, calcium 2-oxalate, trace gypsum, kaolin	ink	outer layer
Tang	2	17	Red		minium, lead chloride, gypsum, lead hydrochloride	minium	outer layer
Tang	2	18	White		lead sulfate, kaolin, lead white, calcium 2-oxalate	lead sulfate, lead white	outer layer
Tang	2	19	Gold	Pb, Au	lead white, gold powder, trace quartz	gold powder	outer layer
Tang	2	20	Blue		gypsum, calcite, feldspar, quartz, trace gypsum, calcium 2-oxalate	azurite	outer layer
Tang	2	21	Green		malachite, lead white, quartz, trace gypsum	malachite	outer layer
Tang	2	22	White	Pb	gypsum, quartz, lead sulfate, trace calcium oxalate	lead sulfate	outer layer
Tang	2	23	Red		cinnabar, trace kaolin, calcite, minium	cinnabar, minium	outer layer
Tang	2	24	Light yellow	Pb	lead white, quartz	lead white	outer layer
Tang	3	25	Red	Pb, Hg	cinnabar, lead sulfate, minium, kaolin	cinnabar, minium	outer layer
Tang	3	26	White		lead sulfate, lead white, quartz, kaolin	lead sulfate, lead white	outer layer
Tang	3	27	Green		atacamite, quartz, trace kaolin	atacamite	outer layer
Tang	3	28	Blue-black		gypsum, quartz, calcium 2-oxalate, trace kaolin	azurite	outer layer
Tang	3	29	Gold		lead white, gold powder	gold powder	outer layer
Tang	3	30	Blue	Cu, trace Pb	azurite, quartz	azurite	outer layer
Tang	3	31	White		quartz, calcium 2-oxalate, basic lead sulfate	lead sulfate	outer layer
Tang	3	32	White		lead white, quartz, gypsum	lead white, gypsum	inner layer
Tang	3	33	Red		minium, calcium 1-oxalate, cinnabar	minium, cinnabar	outer layer

Table 1 continued

Tang	3	34	Blue-black	Cu, trace Pb	azurite, quartz	azurite	inner layer
Tang	3	35	Blue	Cu, trace Pb	azurite, quartz	azurite	inner layer
Tang	3	36	Green		malachite	malachite	inner layer
Tang	3	37	Red		minium, gypsum	minium	inner layer
Tang	3	38	Red	Pb, Hg	cinnabar, quartz, trace minium, lead white, kaolin	cinnabar, minium	outer layer
Tang	3	39	Brown-black	Pb	minium, quartz, calcite, lead hydrochloride, lead oxide	minium, lead oxide	inner layer
Tang	3	40	Gold		lead white, gold powder, gypsum	gold powder	inner layer
Tang	3	41	Red	Pb, Hg	cinnabar, minium, gypsum	cinnabar, minium	inner layer
Tang	3	42	Green		malachite, gypsum, quartz, lead white	malachite	inner layer
Tang	3	43	Light green	Pb, Au	malachite, lead white, trace quartz	malachite	inner layer
Tang	3	44	White		kaolin, gypsum, trace quartz, lead sulfate, mica	kaolin, gypsum	outer layer
Tang	3	45	Black		quartz, calcium 2-oxalate, basic lead sulfate	ink	outer layer
Tang	3	46	White	Pb	lead white	lead white	same layer
Tang	3	47	Blue		minium, cinnabar, kaolin, quartz		outer layer[b]
Tang	3	48	Red		minium, cinnabar, calcite, trace kaolin	cinnabar, minium	outer layer
Tang	3	49	Dark green		malachite, lead white, quartz	malachite	outer layer
Tang	3	50	Light green		malachite, lead white, quartz, trace calcite, lead sulfate, calcium 2-oxalate	malachite	outer layer
Tang	3	51	Gold	Au, Pb	gold powder, lead white	gold	outer layer
Tang	3	52	Gold	Au, Pb	gold powder, lead white	gold	outer layer
Tang	3	53	Red		cinnabar, minium, quartz, trace calcium 2-oxalate	cinnabar, minium	outer layer
Tang	3	54	Brown	Pb	calcium 2-oxalate, leas sulfate, mica, quartz, minium, lead oxide		outer layer
Tang	3	55	Pink		lead sulfate, quartz, cinnabar, minium, trace mica calcium 2-oxalate	cinnabar, minium	outer layer
Tang	3	56	Red		cinnabar, minium, lead sulfate	cinnabar, minium	outer layer
Tang	3	57	Light green		quartz, lead sulfate, trace malachite, gypsum	malachite	outer layer
Tang	3	58	Blue		azurite, quartz, calcite, feldspar	azurite	outer layer
Tang	3	59	Black		calcite, feldspar, gypsum	ink	outer layer
Tang	3	60	White		lead sulfate, lead white	lead sulfate, lead white	outer layer
Tang	3	61	White		gypsum, anhydrite, lead white	gypsum, anhydrite, lead white	inner layer
Tang	2	62	Black		gypsum, lead white, quartz, feldspar	ink	inner layer
Tang	2	63	Red		cinnabar, gypsum, anhydrite, lead white	cinnabar	inner layer
Tang	2	64	Blue		lead white, azurite, quartz	azurite	inner layer
Tang	2	65	Green		paratacamite, gypsum, quartz, malachite	paratacamite	outer layer
Tang	2	66	Black		quartz, calcium 2-oxalate, lead sulfate, trace gypsum, kaolin, feldspar	ink	outer layer
Tang	3	67	Green		atacamite, calcite, quartz	atacamite	outer layer

Table 1 continued

Tang	3	68	Red		kaolin, gypsum, trace quartz, lead sulfate, mica	cinnabar, minium	outer layer
Tang	3	69	Brown	Pb	quartz, calcium 2-oxalate, basic lead sulfate	minium, lead oxide	inner layer
Tang	3	70	Green	Cu, trace Pb	malachite, gypsum, calcium 2-oxalate	malachite	inner layer
Tang	3	71	White		gypsum, trace cinnabar	gypsum	inner layer[c]
Tang	3	72	Red		gypsum, cinnabar	cinnabar	inner layer
Tang	3	73	Blue	Cu, Ni, trace Pb	azurite, gypsum	azurite	inner layer
Tang	3	74	Black		gypsum	ink	inner layer
Tang	3	75	Green	Cu, trace Pb	gypsum, malachite, quartz	malachite	inner layer
Tang	3	76	White	Pb	lead white, gypsum	lead white, gypsum	inner layer
Tang	8	77	Black	Pb, Fe	gypsum, trace hematite	ink	outer layer
Tang	8	78	Red	Fe	gypsum, quartz, trace hematite, calcium 2-oxalate	hematite	outer layer
Tang	8	79	White	trace Pb, Fe	gypsum	gypsum	outer layer
Ming	2	80	Green		atacamite, hydrated basic copper chloride, calcite	atacamite, paratacamite	
Ming	2	81	White		kaolin, gypsum, anhydrite, calcium 1-oxalate	kaolin, gypsum, anhydrite	
Ming	2	82	Red		cinnabar, minium, lead hydrochloride	cinnabar, minium	
Ming	2	83	Green		atacamite, paratacamite, calcium 2-oxalate	atacamite, paratacamite	
Ming	2	84	Red		cinnabar, quartz, trace kaolin, calcium 2-oxalate	cinnabar	
Ming	2	85	White		gypsum, kaolin, quartz trace calcite, mica, calcium 2-oxalate, lead hydrochloride	gypsum, kaolin	
Ming	2	86	Black		quartz, kaolin, gypsum, mica, calcium 2-oxalate	ink	
Ming	3	87	Blue	Fe	gypsum, calcium 2-oxalate, quartz		see note[d]
Ming	3	88	Red		minium, cinnabar, calcite, kaolin	minium, cinnabar	
Ming	3	89	Green		malachite, quartz, calcite, gypsum, calcium 2-oxalate	malachite	
Ming	3	90	Black		gypsum, kaolin, quartz, calcium 2-oxalate	ink	
Ming	3	91	White		gypsum, calcium 2-oxalate, lead hydrochloride	gypsum, lead hydroxychloride	
Ming	3	92	Blue	Cu, trace Pb	azurite, calcite, quartz	azurite	
Ming	3	93	Green	Cu, trace Pb	atacamite, hydrated basic copper chloride	atacamite, paratacamite	
Ming	3	94	Red	Pb, trace As	minium, kaolin, trace lead white, calcium 2-oxalate	minium	
Ming	3	95	White	Pb	lead sulfate, trace gypsum, kaolin	lead sulfate	
Ming	3	96	Light yellow	As, trace Pb	gypsum, trace kaolin, calcium 2-oxalate, orpiment	gypsum, kaolin, orpiment	

---

[a] Repainted Tang statues, age of outer layer unknown; all the pigments labeled outer/inner layer belong to this case.

[b] Pigment sample 47 is blue. However, the pigment layer is very thin; part of red pigment sample 48 was incorporated during sampling, and no blue color phase was detected.

[c] Red pigment was mixed in sample 71 during sampling.

[d] No colored phase was detected.

Records of the use of malachite occur in ancient books about painting. Different types of basic copper chlorides probably were the "copper green" pigment recalled by many ancient and modern artists. Copper green is a mineral pigment that is made by artificial methods, and different types may result from different methods of manufacture.

In the Tiantishan grottoes, white pigments containing large quantities of lead were found covering large areas of the paintings. Five types of lead-containing white pigments were identified: lead white, lead sulfate, lead hydroxychloride, lead chloride, and leadhillite. Lead white and lead sulfate were the most commonly used. Gypsum, chalk, anhydrite, and kaolin were also used as white pigments. This extensive use of lead-containing white pigments in grotto wall paintings is rarely seen. It is surmised these pigments were obtained in the region of the Tiantishan grottoes.

There are many different kinds of lead white. The authors have found $PbCO_3 \cdot Pb(OH)_2$; $3PbCO_3 \cdot 2Pb(OH)_2 \cdot H_2O$; $PbCO_3 \cdot Pb(OH)_2 \cdot H_2O$; $2PbCO_3 \cdot Pb(OH)_2$; and $2PbCO_3 \cdot Pb(OH)_2 \cdot H_2O$ in the Mogao grottoes, the Chengde Summer Villa, the Han Tomb in Shou County, Anhui Province, and the wooden pagoda of the Western Xi Tomb in Baoji (Zhou 1990). Lead sulfate was also discovered in one sample from the Mogao grottoes and one sample from the Maijishan grottoes (Xu, Zhou, and Li 1983; Joint Committee on Powder Diffraction Standards, n.d.). Fourteen of ninety-four pigment samples collected in the Tiantishan grottoes contained lead sulfate, which constitutes a major characteristic of the grotto. Basic sulfate and carbonate of lead, the natural mineral leadhillite (Zhou 1991); and lead hydroxychloride, $Pb(OH)_2 \cdot PbCl_2$, which is also the natural mineral laurionite, are two recently discovered natural white pigments used in ancient paintings.

Cinnabar and minium, and mixtures of cinnabar and lead white—or cinnabar, minium, and lead white (or other pigments containing lead)—were present in many red pigment samples. No signs of discoloration were seen.

The brown color found in Cave 3 was identified as a mixture of lead dioxide and minium. Lead dioxide is the oxidation product of minium.

Conclusions

In this work, the authors analyzed ninety-six samples in five caves of the Tiantishan grottoes and discovered that twenty-four different pigments were used (Table 1). These pigments have the following characteristics:

- Large amounts of white pigment containing lead were used; of these, laurionite and leadhillite were first discovered in this work.
- Many of the samples contained calcium oxalates.
- The green pigments were complex.
- Very few yellow pigments have survived in the polychrome statuary and wall paintings of these grottoes. In this work, the authors obtained only two such samples: no material exhibiting yellow coloration was seen in sample 24, and sample 96 was orpiment.

References

Joint Committee on Powder Diffraction Standards, comp.

n.d. *The Powder Diffraction File.* n.p.

X-ray Diffractometer Users' Association

1983 Pigment analysis of wall paintings of the Yungang grottoes. In *Collected Papers of the X-ray Diffractometer Users' Association* 2.

Xu Liye, Zhou Guoxin, and Li Yunhe

1983 X-ray analysis of the pigments of polychrome statues and wall paintings of the Mogao grottoes, Dunhuang. *Dunhuang Research* 1(1):187.

Zhou Guoxin

1990 *Coating Materials Industry* 4.

1991 X-ray analysis of inorganic pigments of polychrome statuary in the Maijishan grottoes. *Kaogu* 8.

Lead Isotope Analyses of Some Chinese and Central Asian Pigments

Robert H. Brill, Csilla Felker-Dennis, Hiroshi Shirahata, and Emile C. Joel

The objective of this article is to encourage conservators of cave paintings and similar Buddhist works of art to take advantage of lead isotope analysis as an adjunct to other scientific investigations of pigments. Based on the exploratory findings reported here, it is expected that such analyses will prove helpful for classifying pigments and for learning more about their geographical origins. In a broader sense, these analyses might also serve as a prelude to a more general study of leads in Central Asian artifacts.

Lead isotope analyses can be carried out on very small samples of lead-containing materials because only microgram quantities of lead are needed. Even samples left over from other examinations, such as X-ray diffraction, are suitable for analysis. Thus, it is often possible to gain useful information without sacrificing additional samples of materials that have already been studied.

Lead Isotope Analysis

For these studies, lead is extracted from minute samples of any lead-containing material or artifact and is analyzed by mass spectrometry. The resulting isotope ratios are compared with ratios determined for other artifacts and for galena (lead sulfide) ores from ancient mining regions. Lead ores from different deposits can vary isotopically, depending on the geological ages of the deposits and the ore genesis. The objects analyzed can be classified by grouping those containing leads that might have a common geographical origin and separating those that contain leads from different mining regions. Judiciously interpreted, these findings offer valuable clues as to where the objects or materials themselves might have been made. In the most favorable instances, the actual mining regions from which the leads came can be identified.

Two complications of the method lie in overlapping and mixing. *Overlapping* refers to the fact that lead ores from different mining regions sometimes have very similar isotope ratios. *Mixing* means that when leads from different sources are recycled and melted together, the resulting isotope ratios fall somewhere between those of the starting leads. Lead isotope ratios are not affected by the chemical history of the parent materials, providing that no contamination with lead from other sources is introduced. Unlike chemical compositions, which are greatly altered by the chemical reactions of processing, manufacturing, and weathering, lead isotope ratios determined today in ancient materials are exactly the same as they were in the original ores mined in antiquity.

Figure 1 summarizes the results of some twelve hundred ancient lead-containing materials, artifacts, and ores from a wide variety of places and times. The ellipses labeled L, M, E, J, and S are reminders of which isotopic ranges correspond—generally—to which sources of lead. L represents ores from the Laurion mines in Greece and artifacts of known Greek origins; M represents leads from Mesopotamia and some from Iran; E, English and certain European ores; J, some ores and artifacts from Japan; and S, leads from Spain, Wales, and Sardinia. Egyptian and Chinese leads are labeled accordingly. Recent research has established that lead isotope analyses are especially useful for studying Chinese and other Asian artifacts, including glasses, bronzes, Chinese blue and Chinese purple pigments, and glazes (Brill, Barnes, and Joel 1991; Brill and Shi et al. 1991; Yamasaki and Murozumi 1991; Brill 1993; Lee, Brill, and Fenn 1991; Brill and Vocke et al. 1991). As can be seen from the ellipses in Figure 1, numerous Chinese leads fall at the upper and lower extremes of the graph (although there are also many in the middle ranges). As more data are collected for ores in China and Central Asia, the locations of the mines that produced these leads should be identified (Brill and Chen 1991).

Figure 1
Summary of lead isotope data for approximately twelve hundred ancient artifacts and galena ores. Points represent samples in the present study. Data are assembled from various publications by one of the authors (RHB).

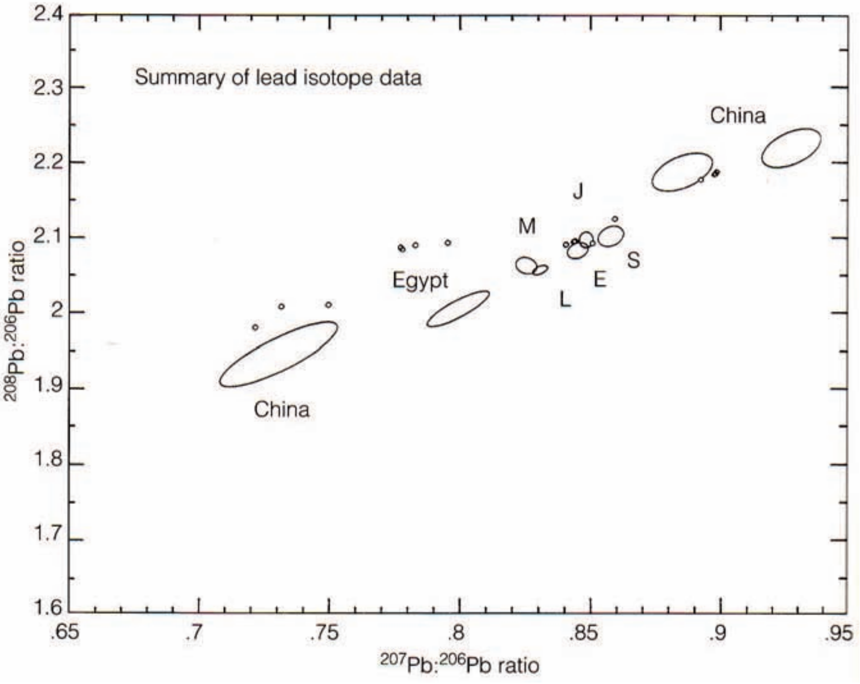

Lead Isotope Analyses of Some Buddhist Pigments

Lead isotope analyses should shed light on questions related to chronological or stylistic differences among Buddhist cave paintings and might distinguish between original and repainted parts of individual works. In this exploratory study, only seventeen pigments have been analyzed, but other analyses are already under way. The analyses were carried out in two laboratories. Some samples were analyzed by Hiroshi Shirahata and his coworkers at the Muroran Institute, while the others were analyzed at the National Institute of Standards and Technology by Emile C. Joel. The results are reported in Table 1 and plotted in Figures 1 and 2, along with the data for other relevant artifacts.

Seven samples from relief wall paintings presently in the Fogg Art Museum were analyzed first. The reliefs date from the Western Wei dynasty (535–557 C.E.) and originally came from two small caves at Tien Lung Shan in Shanxi Province. The pigments were investigated by Csilla Felker-Dennis while she was carrying out conservation examinations in 1982 (Felker and Dennis 1982). Several of the painted areas were found to contain lead in the form of plattnerite, PbO$_2$.[1] All seven samples measured less than 1 mm in their greatest dimension. Because they came from recessed parts of the carving, the samples were believed to represent original sixth-century painting, not later overpainting. Although black today, the pigment might well have originally been red lead (Pb$_3$O$_4$). An alternative hypothesis is that black plattnerite might have been a naturally occurring mineral.

Eight samples of red and white phases from extremely minute flakes of paint from Cave 6 at Yungang were also analyzed. These samples were left over from very comprehensive analyses of the original flakes of paint by Francesca Piqué, who provided the samples for the lead isotope analysis (Piqué herein).

Figure 2
Lead isotope data for thirty-six samples in this study. Data are plotted as large symbols for greater legibility.

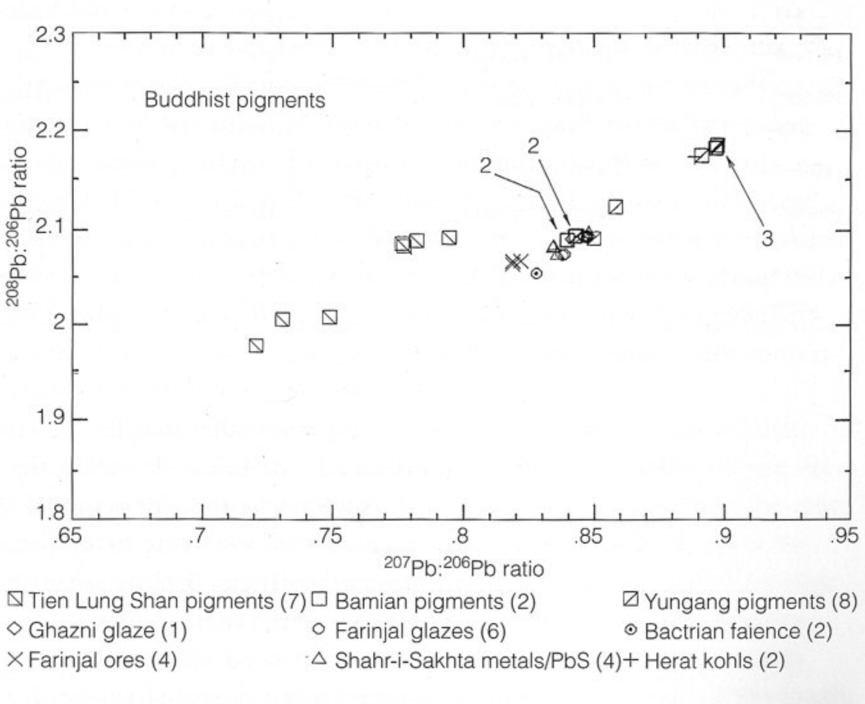

Table 1 Results of lead isotope analyses

Samples are listed in approximate ascending order of $^{207}Pb:^{206}Pb$ ratios.

Sample no.	Description	$^{208}Pb:^{206}Pb$	$^{207}Pb:^{206}Pb$	$^{204}Pb:^{206}Pb$	Lab
Pb-2034	Tien Lung, pigment	1.98001	0.72123	0.04429	NIST
2036	″ ″ ″	2.00771	0.73127	0.04512	″
2035	″ ″ ″	2.01000	0.74946	0.04650	″
2031	″ ″ ″	2.08636	0.77704	0.04858	″
2030	″ ″ ″	2.08372	0.77781	0.04871	″
2032	″ ″ ″	2.08925	0.78279	0.04900	″
2033	″ ″ ″	2.09243	0.79526	0.04997	″
Pb-839	Farinjal, ore	2.06763	0.81933	0.05210	Muro.
838	″ ″	2.06475	0.81935	0.05223	″
840	″ slag	2.06787	0.81950	0.05214	″
837	″ ore	2.06797	0.82250	0.05241	″
Pb-2054	Bactria, faience	2.05534	0.82857	0.05292	″
Pb-1430	Sh.-i-Sok., ingot	2.08146	0.83496	0.05333	″
1431	″ ″	2.08240	0.83514	0.05329	″
1433	″ Ag alloy	2.07408	0.83664	0.05341	″
Pb-1343	Herat, *sormah*	2.08020	0.83588	0.05328	NIST
Pb-841	Farinjal, glaze	2.07420	0.83865	0.05358	Muro.
847	″ ″	2.07506	0.83949	0.05365	″
Pb-2042	Bamian, pigment	2.08965	0.84040	0.05363	NIST
2043	″ ″	2.09013	0.84054	0.05346	″
Pb-1599	Ghazni, glaze	2.09117	0.84226	0.05362	″
Pb-2093	Yungang, pigment	2.09384	0.84341	0.05371	Muro.
2092	″ ″	2.09474	0.84409	0.05382	″
Pb-2055	Bactria, faience	2.09432	0.84705	0.05416	″
Pb-843	Farinjal, glaze	2.09270	0.84688	0.05398	″
846	″ ″	2.09277	0.84773	0.05428	″
842	″ ″	2.09495	0.84811	0.05420	″
845	″ ″	2.09261	0.84828	0.05405	″
Pb-1435	Sh.-i-Sok., galena	2.09679	0.84873	0.05437	″
Pb-2095	Yungang, pigment	2.09183	0.85061	0.05464	″
2099	″ ″	2.12422	0.85915	0.05508	″
Pb-867	Herat, *sormah*	2.17510	0.88955	0.05762	NIST
Pb-2094	Yungang, pigment	2.17641	0.89228	0.05784	Muro.
2097	″ ″	2.18364	0.89742	0.05828	″
2098	″ ″	2.18433	0.89788	0.05831	″
2096	″ ″	2.18689	0.89829	0.05824	″

Two other samples, collected by Brill in 1968, came from niches on the inside east wall near the top of the large Buddha at Bamian. Because of the complex nature of the material, and because some of the material was lost in the 1972 Corning flood, the exact nature of the pigments containing the lead are uncertain. Emission spectrography, X-ray fluorescence (XRF), and X-ray diffraction analyses had been carried out before the flood, along with certain microchemical spot tests. One sample apparently consisted primarily of crushed lapis lazuli and the other of a red pigment, most likely cinnabar (HgS), but red lead could also have been present. Both samples contained a substantial level of lead, but its chemical form was uncertain, and the lead could have been in either a primary pigment or a white ground.

In addition, samples of other materials that might have a bearing on the interpretation of the pigment samples have also been analyzed. These include surface finds from the ancient metallurgical workings at Farinjal, Afghanistan (ores, slags, and lead-glazed pottery shards); blue glazes from two Bactrian faience beads; a glazed terra-cotta animal acquired in Ghazni; metals from Shahr-i-Sokhta; and, from Herat, two modern samples of galena, probably intended for use as the eye cosmetic *sormah*. Several copper-based alloy artifacts from Bamian and/or Chakhcharan are also now being analyzed.

Results of the Analyses

There are two noteworthy observations about the Tien Lung Shan pigments. First, although the seven leads were spread out over a wide isotopic range, all of them fall in the lower range of isotopic values. Three somewhat resemble the leads in the ellipse of Chinese glasses that anchors that corner of the graph in Figure 1. Among the other four samples, only two are isotopically quite similar, while the other two are nearby. Clearly, more than one source of lead is involved, and mixing has probably occurred. Beyond that, it is difficult to interpret the findings, because there does not appear to be any obvious correlation between the data and the locations from which the samples were taken within the cave. Perhaps some repainting is, after all, involved.

The Tien Lung Shan leads are a new type of lead to us. Except for the Chinese glasses, the authors know of no parallels. It is also worth noting that the pigments are displaced somewhat above the general trend of the Chinese data.

One useful inference can be drawn from the wide dispersion of the seven samples. If these pigments had been made from naturally occurring mineral deposits of plattnerite, they most likely would have come from a single, possibly local, deposit—but this is clearly not the case. Instead, the authors feel that the observed variability is more consistent with the view that this plattnerite is not a naturally occurring mineral, but that it is a weathering product of red lead, and that the red lead pigments are synthetic compounds prepared from leads that came from different places. Thus, the data suggest to us that the painted regions now containing black plattnerite were originally red.

The two Bamian pigments, one red and one blue, are virtually identical to one another isotopically, and are markedly different from the Tien Lung Shan pigments (Fig. 2). This is not surprising because the sites are located almost three thousand miles away from each other, but the data also indicate that their leads came from different geological settings.

The leads in the eight Yungang pigments are entirely different from the Tien Lung Shan pigments, and show some variability among themselves. Four of the samples lie in the upper right corner of the graph, having very high isotope ratios. Their leads are similar, but not identical, to those in Warring-States and Han-dynasty Chinese glass eye-beads. Two other Yungang pigments (both red) are not very different from the Bamian pigments, while another—known, from dissection under the microscope, to contain a mixture of both red and white phases—lies between them. The Yungang pigments contain leads that clearly came from at least two different ore deposits.

This brings us, if only fortuitously, to a central point of this discussion. Although only a few samples have been run, they strikingly illustrate that a wide isotopic variability exists among these pigments. They spread over almost the entire range of isotope values encountered in more than twenty years of previous analyses. Seen from one point of view, this is encouraging: it establishes that marked differences exist among pigments from at least some sites, even though this is tempered by the fact that the Tien Lung Shan data alone show a great deal of variability. It remains to be seen whether the variability within other groups of related samples may be smaller (as it is with the two Bamian samples and some of the Yungang samples), so the method will produce the specificity needed to make it useful.

The only way to test for this usefulness is to analyze sets of carefully selected, well-studied, well-documented samples that may become available. That, as stated at the outset, was the principal aim of this writing and the presentation on which it was based: namely, to urge all those connected with research on Buddhist paintings to set aside samples for lead isotope analysis whenever possible.

Some Final Thoughts

Central Asia not only had, and has, its own indigenous cultures, but it also bears the imprints of contacts with innumerable other cultures, both neighboring and far distant. As people came, so also came goods, materials, and technologies. Lead isotope studies might someday be used as a complement to other kinds of evidence for tracing the origins of artifacts or materials that might otherwise remain in doubt. To attempt this, it is necessary first to see whether there is anything such as a Central Asian pattern of lead isotope ratios that might be distinguishable from, for example, the leads of Iran, China, India, and so on.

Unfortunately, limitations of space do not permit a discussion of the results of the initial twenty or so Central Asian artifacts mentioned here, but the data are included in Table 1 and plotted in Figures 2 and 3. Interested readers will be tempted to see a single Central Asian type of lead emerging near the center of Figure 2, but—plotted on an expanded scale, as in Figure 3—that “group” becomes resolved into perhaps as many as a half dozen different mining regions. Readers who are more interested still might like to discover for themselves some of the tantalizing similarities among groups and pairs of samples plotted in Figure 3. Only time, and a lot more data, will tell whether the picture can be clarified or whether—as has happened before—it will all become too entangled to unravel. In any event, that should not impede research on Buddhist pigments, because they

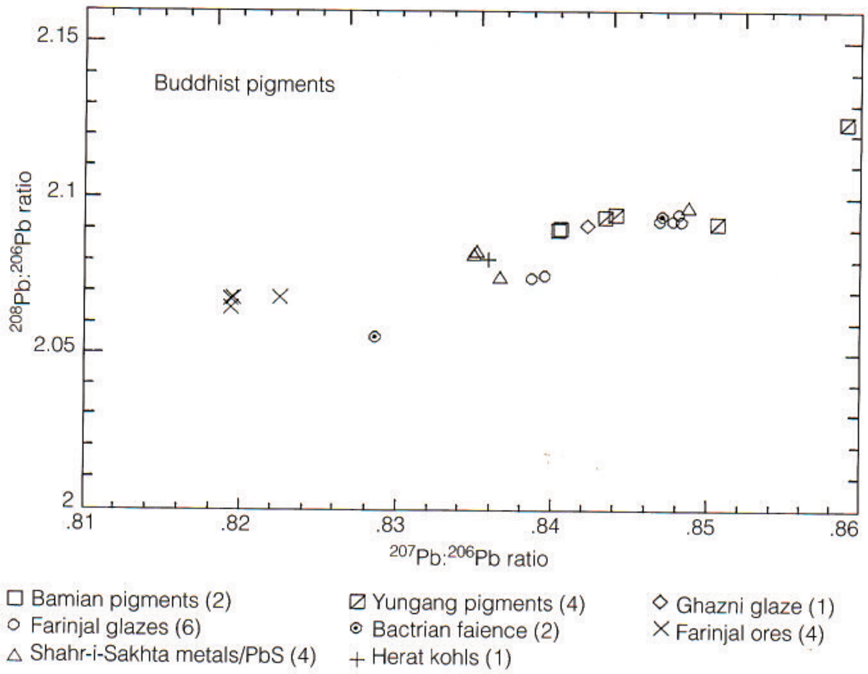

Figure 3
Expanded portion of Fig. 2. Data are plotted as large symbols for greater legibility.

can still be classified relative to one another in a self-contained way and may help art historians and archaeologists to establish connections between paintings found hundreds or even thousands of miles apart.

One of the authors (Shirahata) has recently completed analyses of twelve additional pigments from cave paintings. These are plotted in Figure 4, along with seventeen of the pigments plotted in Figure 2. Further details are available from the authors.

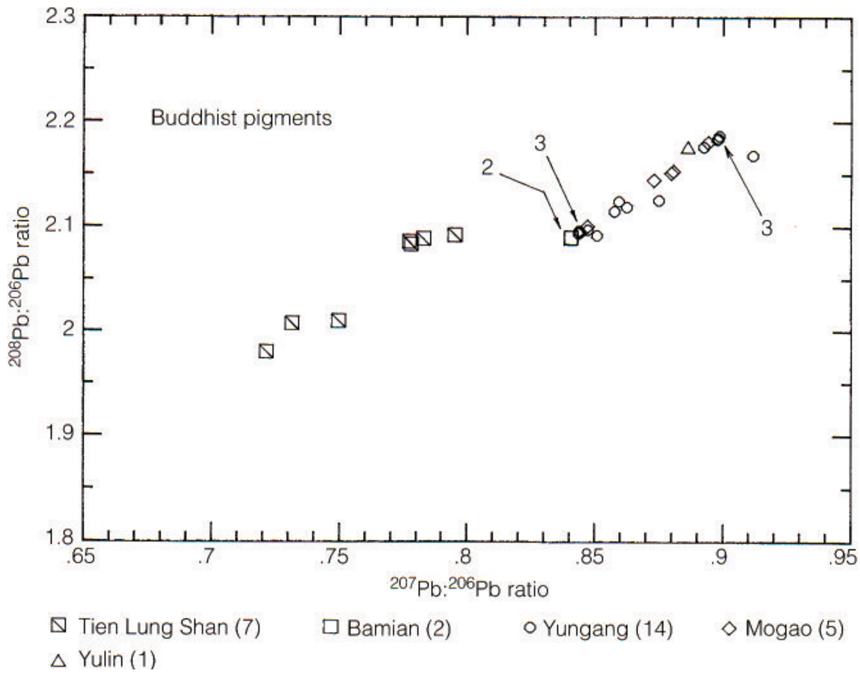

Figure 4
Data for twelve additional pigments from cave paintings (not described in text), along with replotted data for the seventeen pigments in Fig. 2.

Acknowledgments

Special thanks are extended to the individuals and institutions who provided the samples used in this study. They are identified in the sample description section at the end of this chapter. The authors also thank Kazuo Yamasaki, John Dennis, Eugene Farrell, Richard Newman, and Sherri Seavey for their contributions to this research. The diffraction patterns were run by Bryan R. Wheaton of Corning, Inc.; and the X-ray fluorescence by Philip M. Fenn of Corning, Inc., and George J. Reilly, then of the Winterthur Museum.

Note

1 The identification as plattnerite was made by one of the authors (CF-D), in collaboration with John Dennis. It was based on X-ray diffraction and microscopic examinations. At that time the name apsara black was suggested for the pigment. A straightforward calculation (by RHB) shows that the free energy of the reaction, as given here, is about $-40.50\ \text{kJmol}^{-1}$ (at 20 °C), indicating that the red-to-black transformation is thermodynamically favorable ($-40.50\ \text{kJmol}^{-1} = -9.68\ \text{k cal. mol}^{-1}$):

$$Pb_3O_{4(c)} + O_{2(g)} \rightarrow 3PbO_{2(c)}$$

The free energy at 0 °C ($-44.27\ \text{kJmol}^{-1}$) is more negative than that at 35 °C ($-37.70\ \text{kJmol}^{-1}$), suggesting that the color change might tend to go faster in the winter than in summer, although that does not take into account catalysis or factors such as the presence of moisture that could also affect the mechanism and/or rate of reaction.

Sample Descriptions

Tien Lung Shan pigments

This group of samples came from painted stone reliefs now in the Fogg Art Museum. They are traces of pigments from low-relief paintings on the sandstone ceilings of Caves 2 and 3 at Tien Lung Shan in Shanxi Province. Six of the paintings depict apsaras in various attitudes and with various attributes. The seventh (Pb-2036) is a stela depicting the Buddha. All date from the Western Wei dynasty (535–557 C.E.).

Pb-2030	Flake of black pigment with white gypsum (?) ground. The pigment is now plattnerite, a black lead oxide (PbO_2). Cave 2, south. FAM no. 1943.53.9.
Pb-2031	As above. Cave 3, south. FAM no. 1943.53.10.
Pb-2032	As above. Cave 2, east. FAM no. 1943.53.12.
Pb-2033	As above. Cave 3, west. FAM no. 1943.53.14 (14/1).
Pb-2034	As above. Another sample (14/11).
Pb-2035	As above. Another sample (14/14).
Pb-2036	As above. Cave 3, Buddha figure in stone. FAM no. 1943.53.17.

Yungang, China, pigments

These samples were provided by Francesca Piqué. They are remains from analyses described in her article herein.

Pb-2092	Red pigment separated from Piqué no. 11.
Pb-2093	Red pigment separated from Piqué no. 21.
Pb-2094	White pigment separated from Piqué no. 35.
Pb-2095	White pigment separated from Piqué no. 37.
Pb-2096	Red pigment separated from Piqué no. 42.
Pb-2097	White pigment separated from Piqué no. 42.
Pb-2098	Black layer (with some white phases) separated from Piqué no. 44.
Pb-2099	Red pigment (with slight contamination of white phases) separated from Piqué no. 46.

Bamian pigments

Pb-2042	Blue pigment (powdered lapis lazuli) applied to grass-reinforced mud plaster. From wall painting in niche near top of large Buddha. Probably from seventh to ninth century. BAM-1. Collected by RHB on 6 August 1968. Sample contaminated with whitish ground (gypsum) and mud plaster.
Pb-2043	As above, red pigment. BAM-3.

Farinjal, Afghanistan, pigments

These pigments are from specimens collected by RHB on 6 August 1968 at site no. 4 of the National Geographic Society Metallurgical Expedition, headed by Theodore Wertime. This metallurgical site is thought to have been worked from 300 to 1200 C.E. Ore-bearing rock is present.

Pb-837	Mineral phase is black with fine-grained, lustrous crystals.
Pb-838	As above; a similar specimen.
Pb-839	As above; a similar specimen.
Pb-840	As above. Large nugget of vitreous slag. Black (v. dark olive).
Pb-841	As above. Pottery shard. Green glaze over white slip on salmon-colored body. 30–50% PbO.
Pb-842	As above. Bluish green glaze on salmon-colored body. 30–50% PbO.
Pb-843	As above. Green glaze on salmon-colored body. 1–3% PbO.
Pb-845	As above. White glaze on thick buff-colored body. 30–50% PbO.
Pb-846	As above. Rim fragment. White glaze with dark blue, linear, cloudlike decoration on soft, light-gray body. Probably made in Iran in imitation of Chinese porcelain. Said by D. B. Whitehouse to be of a type commonly found near Kandahar. 0.03–0.1% PbO.
Pb-847	As above. Body fragment. White glaze on one surface, mainly dark blue (with some white) on other. Probably made in Iran in imitation of Chinese porcelain. 0.01-0.03% PbO.

Shahr-i-Sokhta, Iran, pigments

The following samples were submitted by Maurizio Tosi of the Istituto Universitario Orientale, Naples, on 29 June 1977.

Pb-1430	Pan-shaped ingot, from bottom of a melting crucible, ca. 2500 B.C.E. XRF gives 75% Pb, no Cu or Sn.
Pb-1431	As above; a similar ingot. XRF gives 75% Pb, no Cu or Sn.
Pb-1433	As above. A stamp seal; 2500–2000 B.C.E.
Pb-1435	As above. A piece of galena; 2200–1800 B.C.E. Square RWJ(L).

Other pigment samples

Pb-1599	Glazed terra-cotta figure of an animal; date uncertain. Purchased in Ghazni by Robert H. Brill on 10 August 1968. Sample is of green lead glaze.
Pb-2054	Faience bead in the shape of a duck. Bactria. Ancient but of uncertain date. Whitish, porous, fine-grained body with remains of greenish-blue glaze. From same group as CMG 93.7.1. Sample consists of glaze with much body material. PbO ~ 0.08% in glaze.
Pb-2055	An incurved biconical bead, with perforated bore (not of the hollow nutshell type). Bactria. Whitish, porous, fine-grained body with remains of blue glaze. From same group as CMG 93.7.1. Sample consists of glaze with much body material. PbO ~ 0.03% in glaze (related to sample Pb-2054).
Pb-867	Herat, Afghanistan. Nugget of galena purchased in the potters' bazaar. Possibly for use as *sormah,* an eye cosmetic. See Brill's field notes for 2 July 1972.
Pb-1343	Herat, Afghanistan. Said to be from Chakhcharan. Galena, possibly for use as *sormah,* an eye cosmetic (related to sample Pb-867). See Brill's field notes for 15 September 1977.

References

Brill, Robert H.

1993 Scientific investigation of ancient Asian glass. In *Nara Symposium '91 Report: Unesco Maritime Route of Silk Roads,* 70–79. Paris: Unesco.

Brill, Robert H., I. Lynus Barnes, and Emile C. Joel

1991 Lead isotope studies of early Chinese glasses. In *Scientific Research in Early Chinese Glass,* ed. R. H. Brill and J. H. Martin, 65–93. Corning, N.Y.: Corning Museum of Glass.

Brill, Robert H., and Margery Chen

1991 A compilation of lead isotope ratios of some ores from China published by Chen Yuwei, Mao Cunxiao, and Zhu Bingquan (partial English translation of original paper in Chinese). In *Scientific Research in Early Chinese Glass,* ed. R. H. Brill and J. H. Martin, 167–80. Corning, N.Y.: Corning Museum of Glass.

Brill, Robert H., Shi Meiguang, Emile C. Joel, and Robert D. Vocke

1991 Addendum to chapter 5. In *Scientific Research in Early Chinese Glass,* ed. R. H. Brill and J. H. Martin, 84–90. Corning, N.Y.: Corning Museum of Glass.

Brill, Robert H., Robert D. Vocke, Jr., Wang Shixiong, and Zhang Fukang

1991 A note on lead isotope analyses of faience beads from China. *Journal of Glass Studies* 33:116–18.

Felker, Csilla Z., and John R. Dennis

1982 Caves at T'ien Lung Shan: A technical study of pigments on stone. Internal report. The Fogg Art Museum, Harvard University, Cambridge, Mass.

Lee In-Sook, Robert H. Brill, and Philip M. Fenn

1991 Chemical analyses of some ancient glasses from Korea. In *Proceedings of the 12th Congress of the International Association for the History of Glass, Vienna, August, 1991,* 163–76. Liege: International Association for the History of Glass.

Yamasaki, Kazuo, and Masayo Murozumi

1991 Similarities between ancient Chinese glasses and glasses excavated in Japanese tombs. In *Scientific Research in Early Chinese Glass,* ed. R. H. Brill and J. H. Martin, 91–98. Corning, N.Y.: Corning Museum of Glass.

Formation and Stability of Chinese Barium Copper–Silicate Pigments

Hans G. Wiedemann and Gerhard Bayer

Blue and purple pigments were used in ancient China for decorating pottery and metallic objects and for wall paintings. They were also produced in the form of octagonal sticks. The use of such pigments was common, especially during the Han dynasty (208 B.C.E.–220 C.E.). West FitzHugh and Zycherman (1983, 1992) showed that these pigments are barium copper silicates of defined, specific composition. This report primarily addresses the two Chinese pigments, Han blue ($BaCuSi_4O_{10}$) and Han purple ($BaCuSi_2O_6$).

Han blue has the identical structure and crystal habit as Egyptian blue ($CaCuSi_4O_{10}$) (Pabst 1959; Chase 1971; Bayer and Wiedemann 1976), a calcium copper silicate produced and used extensively in ancient Egypt beginning around 3000 B.C.E. Previous investigations of the formation and stability of Egyptian blue and its strontium and barium analogues showed that the barium copper silicate is thermally much more stable than Egyptian blue. Compared to the system $CaO\text{-}CuO\text{-}SiO_2$, the corresponding system with BaO is more complex. At least four ternary barium copper silicates have been found to exist (JCPDS files; Finger, Hazen, and Hemley 1989): $BaCuSi_4O_{10}$ (Han blue), $BaCuSi_2O_6$ (Han purple), $BaCu_2Si_2O_7$ (another blue), $Ba_2CuSi_2O_7$ (another blue). Synthesis of the pure phases is not straightforward; usually a mixture of compounds is formed initially, depending on the raw materials used, their ratio, the addition of fluxes, and the temperature and time of reaction.

The role of the barium minerals is of special interest. China has a long history and tradition of developing and utilizing ores and minerals. It is likely that copper sulfides were used together with barite and silica sand or quartzite to make the pigments. Barite ($BaSO_4$) is found in a variety of deposits all over China. Witherite ($BaCO_3$), which is sometimes associated with barite, is much rarer. The raw materials for the blue and purple barium copper–silicate pigments used in the Mogao grottoes probably came from copper deposits in Gansu Province, such as those near Lanzhou, Gulang, or Jiayuguan (Gloria, Harrison, and Braumann 1985).

Synthesis of the barium copper–silicate pigments requires specific conditions with respect to heat treatment and flux addition, depending on the raw materials used. The investigations reported here focused primarily on the effect of the barium minerals on the formation of the blue and purple pigments. For these experiments copper was added as an oxide since any copper sulfide will be oxidized to CuO well below the temperature where the reaction starts (Bayer and Wiedemann 1992). The reaction rate was accelerated by the addition of fluxes such as NaCl and Na_2CO_3. Additional investigations concerned the chemical and thermal stability of the various pigment samples.

Experimental Approach

All the barium copper silicates were prepared by solid-state reaction in air between the corresponding oxides in the temperature range of 900–1100 °C. The raw materials, chemically pure and finer than 40 μ, were $BaSO_4$, $BaCO_3$, CuO, Cu_2S, and SiO_2. They were homogeneously mixed, compacted slightly, and heated for approximately twenty hours.

The crystalline reaction products were identified by X-ray diffraction (Guinier de Wolff camera, CuK-alpha radiation). This proved difficult when a mixture of the various barium copper silicates was present in the samples along with barium silicates and unreacted starting materials.

The Mettler Thermoanalyzer TAl was used for simultaneous thermogravimetry (TG) and differential thermal analysis (DTA). In addition, the Mettler Toledo System TA 8000/TG 850 was used for TG, especially in a controlled atmosphere. The heating rates varied between 2 °C min^{-1} and 10 °C min^{-1}. Platinum and alumina crucibles were used because of their high thermal conductivity, which is important for the DTA runs. Otherwise, any ceramic container can be used for the synthesis of the pigments; in the authors' experience, it has no effect on the color.

Results and Discussion

Synthesis by solid-state reaction was carried out to understand the formation of the different colors of barium copper–silicate pigments. Previous studies of Han blue ($BaCuSi_4O_{10}$) showed that not only temperature but also the barium compound used and the fluxes added (Bayer and Wiedemann 1976) have a distinct effect on the color tone of this pigment.

For the present work, mixtures of different stoichiometry were prepared, using only $BaCO_3$ and $BaSO_4$ to simulate the preparation of the blue and purple pigments with naturally occurring raw materials. Other barium compounds are more reactive; however, it is highly unlikely that they were used in ancient China.

Fluxes posed a particular problem. Their addition had a definite effect on the formation and color of the resulting pigment. It was found that the addition of more than 5% Na_2CO_3, and heating to above 1000 °C, resulted in melting of the Han purple compound to a glass. Han blue was more stable. There were other side reactions from the fluxes. In starting mixtures with $BaCO_3$ as the barium source, the addition of Na_2SO_4 caused the intermediate formation of $BaSO_4$ in the temperature range of 600–800 °C. This was due to the displacement reaction $BaCO_3 + Na_2SO_4 \rightarrow BaSO_4 + Na_2CO_3$ (Bayer and Wiedemann 1987). Since there is a pronounced difference between the reaction behavior of $BaCO_3$ and $BaSO_4$ in the formation of the pigments, the influence of the flux components in the reaction must also be taken into account. Because the original Han purple pigment contained a high proportion of lead oxide, this was also tried as a flux. It was very effective in the formation of both Han purple and Han blue at 900 °C. However, adding more than 5% lead oxide led to partial melting and glass formation above 1000 °C. This agreed with the macroscopic appearance of the obviously partially vitrified purple octagonal sticks (West FitzHugh and Zycherman 1983, 1992).

Synthesis of Han purple and Han blue with $BaCO_3$

To synthesize the purple and blue pigments, mixtures of $BaCO_3$, CuO, and quartz powder were prepared with the following stoichiometric ratios: 1:1:2, 1:1:4, 1:2:2, and 2:1:2. The mixtures were placed in porcelain crucibles, compacted slightly, and heated in air to 900, 1000, and 1100 °C. A flux of 3% Na_2CO_3, or 5% PbO, or 10% NaCl was added to some of these mixtures. TG and DTA runs were carried out with the 1:1:2 and 1:1:4 mixtures. They showed that in the presence of SiO_2, the decomposition of $BaCO_3$ starts below its phase transition at around 800 °C. The decomposition to BaO + CO_2 proceeds faster above this temperature and is complete at about 950 °C (Fig. 1). The solid-state reaction leading to barium copper silicates probably starts around 900 °C. Partial melting and reduction $Cu^{2+} \rightarrow Cu^{1+}$ occur at temperatures above 1050 °C depending on the BaO:CuO:SiO_2 ratio (Fig. 2). Han purple ($BaCuSi_2O_6$) is formed as the primary barium copper silicate in mixtures with the 1:1:4 stoichiometry. It is thermally less stable than Han blue ($BaCuSi_4O_{10}$) and melts with decomposition around 1100 °C. Pure Han blue could be synthesized more easily with the addition of fluxes such as Na_2CO_3 or borax. Section A of Table 1 shows some of the syntheses carried out with $BaCO_3$ and the various phases that formed. The latter were identified by X-ray diffraction.

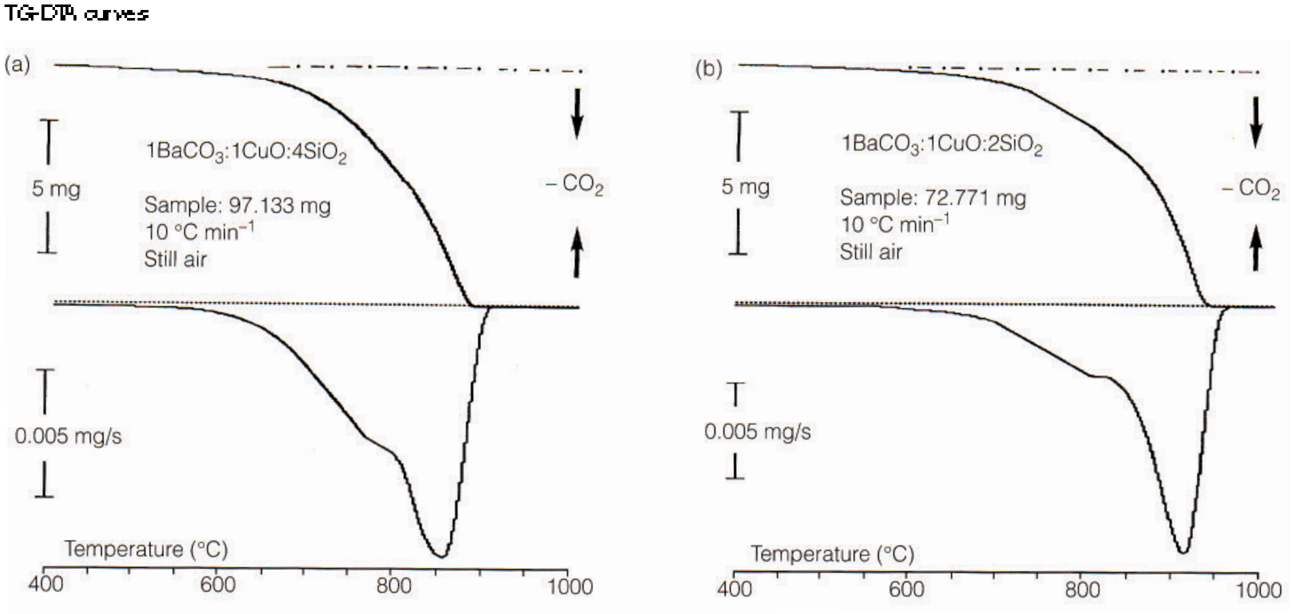

Figure 1
Thermogravimetry (TG) and differential thermal analysis (DTA) curves of $BaCO_3$-CuO-SiO_2 mixtures heated to 1000 °C for the synthesis of Han blue and Han purple.

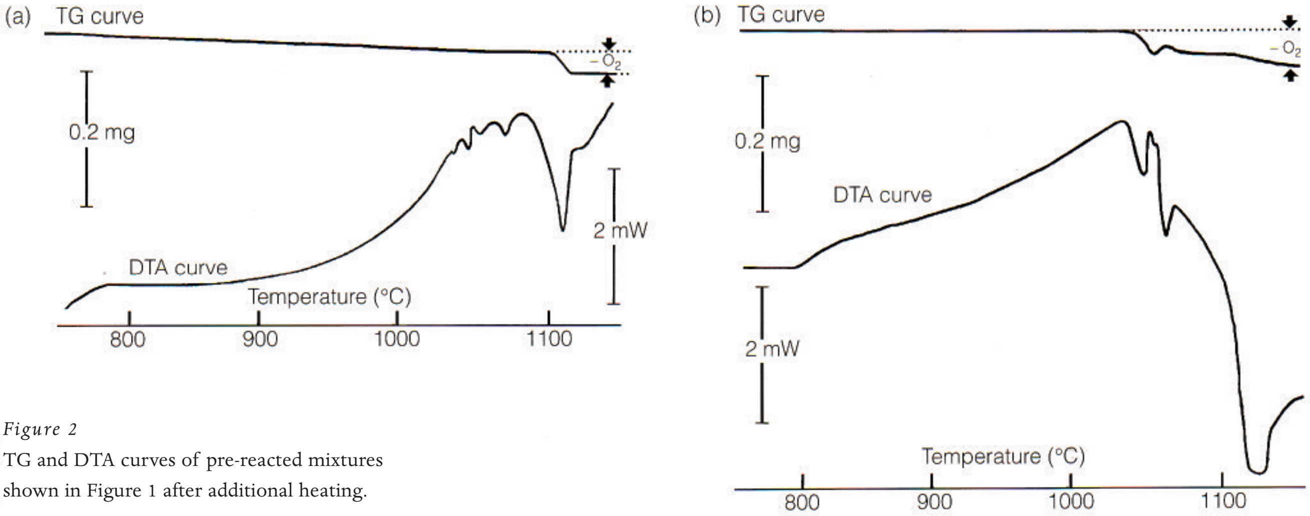

Figure 2
TG and DTA curves of pre-reacted mixtures shown in Figure 1 after additional heating.

Table 1 Synthesis of barium copper–silicate pigments (X-ray diffraction results)

	Reaction products after heat treatment	
Sample mixture	1000 °C, 20 h	1100 °C, 20 h
(A) With $BaCO_3$		
$BaCO_3$, CuO, SiO_2 1:1:2	$BaCuSi_2O_6$ (m) $BaCu_2Si_2O_7$ (w) blue-purple	$BaCuSi_2O_6$ (s) purple
$BaCO_3$, CuO, SiO_2 1:1:2 +3% Na_2CO_3	$BaCuSi_2O_6$ (w) ? (w) purple	$BaCuSi_2O_6$ (s) purple
$BaCO_3$, CuO, SiO_2 1:1:2 +5% PbO	$BaCuSi_2O_6$ (s) $BaCuSi_4O_{10}$ (w) purple-blue	
$BaCO_3$, CuO, SiO_2 1:1:4	$BaCuSi_2O_6$ (s) $BaCuSi_4O_{10}$ (m) bluish-purple	$BaCuSi_4O_{10}$ (s) $BaCuSi_2O_6$ (vw) blue
$BaCO_3$, CuO, SiO_2 1:1:4 +3% Na_2CO_3	$BaCuSi_4O_{10}$ (s) $BaCuSi_2O_6$ (m) blue	$BaCuSi_4O_{10}$ (s) blue
(B) With $BaSO_4$		
$BaSO_4$, CuO, SiO_2 1:1:2	$BaCuSi_4O_{10}$ (m) $BaSO_4$ (m) CuO (vw) bluish-gray	$BaCuSi_4O_{10}$ (s) $BaSO_4$ (m) $BaCuSi_2O_6$ (m) purple-blue
$BaSO_4$, CuO, SiO_2 1:1:2 +3% Na_2CO_3	$BaCuSi_4O_{10}$ (s) $BaSO_4$ (m) bluish-gray	$BaCuSi_4O_{10}$ (m) $BaCuSi_2O_6$ (s) $BaSO_4$ (w) purple-blue
$BaSO_4$, CuO, SiO_2 1:1:2	$BaCuSi_4O_{10}$ (m) $BaSO_4$ (m) CuO (w) greenish-blue	$BaCuSi_4O_{10}$ (s) $BaSO_4$ (w) blue
$BaSO_4$, CuO, SiO_2 1:1:4 +3% Na_2CO_3	$BaCuSi_2O_6$ (s) $BaSO_4$ (m) bluish-purple	$BaCuSi_4O_{10}$ (s) blue

vw = very weak w = weak m = medium s = strong v = very strong

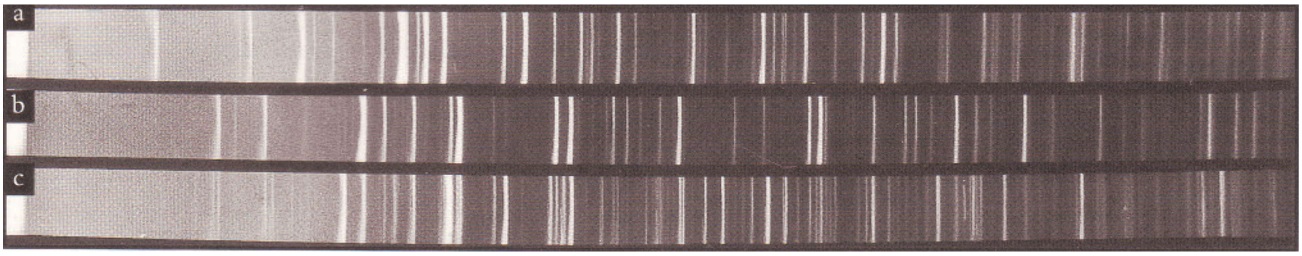

Figure 3
X-ray-diffraction powder patterns of barium copper–silicate pigments, top to bottom: (a) Han blue, (b) Han purple, and (c) $BaCu_2Si_2O_7$ (another blue).

The formation of colorless barium metasilicate as a primary phase was observed in several mixtures. Most of the $BaCO_3$:CuO:SiO_2 mixtures showed the presence of both purple and blue barium copper silicate, especially when heated to around 1000 °C. Pure Han purple was easier to synthesize than pure Han blue. The kind of flux added to the starting mixture, which contained the highly reactive $BaCO_3$, had a strong effect on the resulting color tone, which could be pure purple, pure blue, or a mixture of both. The addition of NaCl caused volatilization of some copper as $CuCl_2$ which is oxidized to CuO in the cooler zone of the furnace. Fluxes such as Na_2CO_3, PbO, or borax did not cause problems. When heating mixtures in which copper sulfides were used, their oxidation led to the evolution of SO_2, which reacted with $BaCO_3$ to form $BaSO_4$. This caused changes in the color tone compared to a mixture of identical stoichiometry where CuO was used instead of Cu_2S. The X-ray-diffraction powder patterns of pure Han purple (1:1:2) and Han blue (1:1:4) are shown in Figure 3.

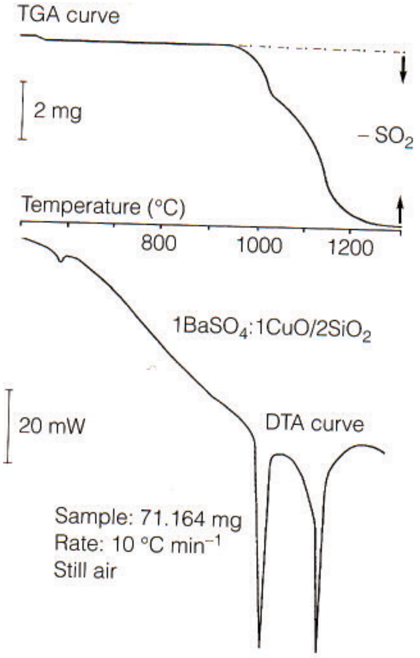

Figure 4
TG and DTA curves of the $BaSO_4$-CuO-SiO_2 mixture for the synthesis of Han purple.

Synthesis of Han purple and Han blue with $BaSO_4$

For these syntheses, the same procedure used for mixtures containing $BaCO_3$ was followed. TG and DTA runs showed that $BaSO_4$ has a higher thermal stability than $BaCO_3$ and starts to decompose slowly above 950 °C (Fig. 4). Even after heating for twenty hours at 1100 °C, a large amount of $BaSO_4$ remained unreacted. Consequently, the proportion of the Han purple and Han blue reaction products ($BaCuSi_2O_6$ and $BaCuSi_4O_{10}$) differed from the proportion found in corresponding mixtures with $BaCO_3$; hence the color tone also differed. Section B of Table 1 shows some of the syntheses carried out with $BaSO_4$.

The slower decomposition rate of $BaSO_4$, and thus the smaller amount of BaO available for reaction, obviously favored the primary formation of the more silica-rich Han blue. In addition, for the mixture ratio 1:1:2, Han blue continued to persist along with Han purple even at 1100 °C. This is in contrast to the corresponding mixtures with $BaCO_3$, where the formation of Han purple was strongly favored over Han blue, and where reactions generally started at lower temperatures. Mixtures with a 1:1:2 ratio melted to a homogeneous black glass above 1,300 °C and formed thin slabs from around 1,500 °C. Cooling this glass melt slowly in the crucible resulted in a blue-purple reoxidized material containing Han blue and Han purple as crystalline phases (Fig. 5). Reheating of the quenched glass to 950 °C led to crystallization of Han blue in a powdered sample, and crystallization of Han blue, Han purple, and $BaSi_2O_5$ in bulk samples. This difference in recrystallization was due to surface-dependent nucleation.

Thermal and Chemical Stability of Han Purple and Han Blue

Figure 5
Blue-purple pigment mixture recrystallized during cooling of glass melt.

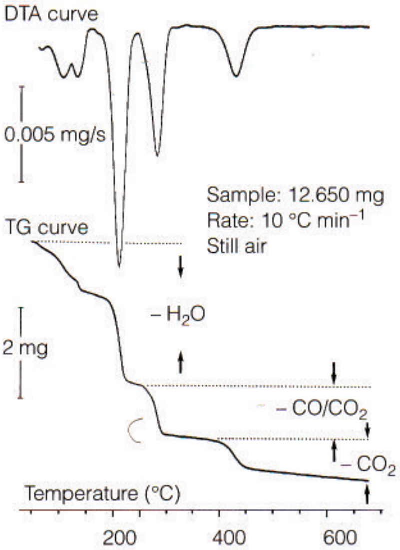

Figure 6
TG and DTA curves of the reaction product from Han purple and oxalic acid.

Han purple and Han blue are closely related structurally (Pabst 1959; Finger, Hazen, and Hemley 1989). Both show the identical square, fourfold coordination for Cu^{2+} and SiO_4^- tetrahedra that are linked to four-membered rings. These rings are isolated in the structure of Han purple but linked to four others in the adjacent layer in Han blue. This leads to the formation of a unique, four-ring, silicate-layer structure for Han blue and a different kind of barium-oxygen coordination. The continuous, zigzag, four-ring layers parallel to the (001) crystal face probably lead to better shielding of the barium and copper ions, and may be responsible for the higher thermal and chemical stability of Han blue over Han purple.

The phase diagram for the $BaO\text{-}CuO\text{-}SiO_2$ system is not yet known. However, both Han purple and Han blue lie on the straight line that runs from $BaCuO_2$ to SiO_2. Therefore, the more silica-rich Han blue ($BaCuSi_4O_{10}$) should have a higher melting point than Han purple ($BaCuSi_2O_6$). This was confirmed by the isothermal heat treatment of corresponding samples at 1200 °C for four hours. Pure Han purple (1:1:2) melted to a viscous, black-green glass, whereas Han blue (1:1:4) only showed increased sintering. X-ray investigation of these samples quenched from 1200 °C proved that the former was amorphous and vitreous, while the latter was unchanged $BaCuSi_4O_{10}$ (Han blue).

The striking difference in chemical stability between the purple and blue pigments has already been stressed by Pabst (1959) and by West FitzHugh and Zycherman (1983), and was confirmed by the authors' experiments. Blue $BaCuSi_4O_{10}$ was completely stable in dilute acids while purple $BaCuSi_2O_6$ faded rapidly and decomposed. The same effect was found when the purple pigment was treated with aqueous oxalic acid. It has been documented that lichens, which excrete oxalates or even oxalic acid, play a role in the deterioration of works of art (Seaward and Giacobini 1989). The turquoise-bluish residue formed by the reaction of Han purple with oxalic acid was identified as the double oxalate $BaCu(C_2O_4)2 \cdot 6H_2O$. Its decomposition to $CuO + BaCO_3$ can be seen from the TG curve shown in Figure 6. Below 250 °C there is a certain similarity to the decomposition of oxalic acid with H_2O, CO, and CO_2 given off. The peaks at higher temperature probably result from the decomposition of intermediate, basic copper carbonates. Additional experiments showed that Han purple also decomposes gradually in an atmosphere containing SO_2.

It was possible to analyze a tiny sample of original Han purple and to compare its composition to that of the synthetic purple pigment (Fig. 7). The excess silica and high lead concentration in the original sample was striking; these materials were obviously added as a flux or sintering aid. To the authors' knowledge, lead isotope analysis has not been performed on the Han purple sticks.

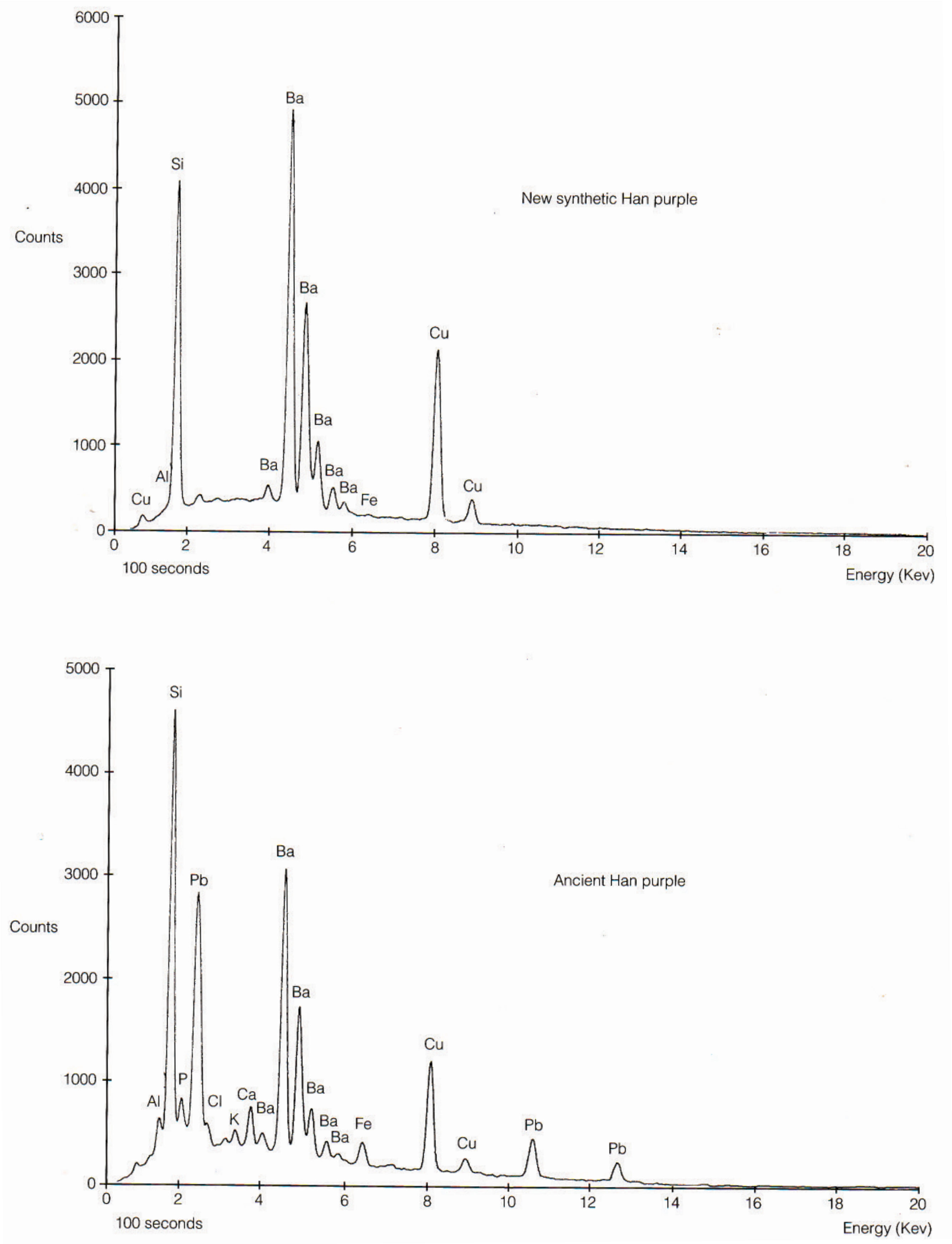

Figure 7
Energy-dispersive X-ray analysis curves of synthetic and ancient Han purple.

Effect of Pigments on the Conservation of Objects

In previous investigations of colored Egyptian papyri, spores and fungi were not observed in areas where Egyptian blue ($CaCuSi_4O_{10}$) was used as pigment. These findings were confirmed by further studies of different papyri. It was therefore assumed that copper-containing compounds had some effect on inhibiting the growth of mold, fungi, and lichens. Experiments with lichen-covered limestone proved this; no further growth occurred in areas where the lichens were removed and the exposed limestone was subsequently painted with Egyptian blue.

It is interesting that the production of "blue bread" is mentioned in documents of the Eighteenth Dynasty (1500 B.C.E.) in ancient Egypt (Sethe 1961). Since the Egyptians produced air-dried bread for emergency situations, it may be that they had some knowledge about the conservation effect of the Egyptian blue pigment. Likewise, it is possible that Han blue and/or Han purple may have similar fungicidal properties as Egyptian blue. Experiments to examine this have begun. A thermomicrobalance and hot-stage microscope are being used to obtain detailed insight into the growth and life cycle of lichens that attack artifacts. This setup makes it possible to correlate weight changes with macroscopic and microscopic changes in the artifacts as a function of different atmospheres and temperatures. The results are important to the understanding of how chemical environment affects the growth and life cycle of lichens, and could lead to new ways of protecting objects from deterioration.

Summary

Experimental investigations were carried out on the synthesis of barium copper–silicate pigments by means of solid-state reactions. It was shown that the main factors that control the color tone of the different purple and blue pigments are kind and purity of raw materials used, mixture ratio, nature of the flux used, heating, and temperature. There was a pronounced difference in reaction behavior between $BaCO_3$ and $BaSO_4$ as starting materials; generally the carbonate reacted much faster and at lower temperature than the sulfate. Han purple ($BaCuSi_2O_6$) was easier to obtain in pure form than Han blue ($BaCuSi_4O_{10}$), unless special fluxes were added. Depending on their chemical composition, the fluxes would react with the raw materials, and this also had an effect on pigment color.

Han blue was thermally and chemically much more stable than Han purple. Heating to 1200 °C did not change blue $BaCuSi_4O_{10}$, while purple $BaCuSi_2O_6$ completely melted to a black glass just below 1100 °C. This glass could be recrystallized to Han purple at about 900 °C. The poor resistance of Han purple to acids (including oxalic acid) resulted in rapid fading and decomposition. This is in striking contrast to the completely stable Han blue. This is probably due to the different coordination of Ba^{2+} and the arrangement of the Si_4O_{10} rings in the structures of these compounds.

In conclusion, the results of these investigations may contribute to a better appreciation of the early Chinese methods of manufacturing Han blue and Han purple pigments, and lead to an explanation for the variety of color tones observed.

Acknowledgments

The authors would like to thank Elisabeth West FitzHugh, Freer Gallery of Art, Smithsonian Institution, Washington, D.C., for providing a small sample of original Han purple.

References

Bayer, G., and H. G. Wiedemann

1976 *SANDOZ Bulletin* 40:20–39.

1987 Displacement reactions in gypsum and in anhydrite. *Thermochimica Acta* 114:75–82.

1992 *Thermochimica Acta* 198:303–12.

Chase, W. T.

1971 *Science and archaeology.* Cambridge: MIT Press.

Finger, L. W., R. M. Hazen, and R. J. Hemley

1989 *American Mineralogist* 74:952–55.

Gloria, H. G, H. Harrison, and F. Braumann

1985 *Bergbau, Rohstoffe Energie.* Vol. 24. 2d ed. Essen: Verlag Glückauf GmbH.

JCPDS Powder Diffraction File No. 12–520, No. 39–253, No. 40–84.

Pabst, A.

1959 *Acta Crystallographica* 12:733–39.

Seaward, M. R. D., and C. Giacobini

1989 Oxalate encrustation by the lichen *Dirina massiliensis* forma *Sorediata* and its role in the deterioration of works of art. In *Oxalate Films: Origin and Significance in the Conservation of Works of Art. Proceedings. Milan, 25–26 October 1989,* 215–19. Milan: Centro CNR Gino Bozza.

Sethe, K.

1961 *Urkunden der 18. Dynastie.* Vol. 3. Berlin: Akademie Verlag; Graz: Verlagsanstalt. Seite IV 638/36.

West FitzHugh, E., and L. A. Zycherman

1983 *Studies in Conservation* 28:15–23.

1992 A purple barium copper silicate pigment from early China. *Studies in Conservation* 37(3):145–54.

The Polychrome Terra-cotta Army of the First Emperor Qin Shi Huang

Wu Y. Onggi, Zhou Tie, Zhang Zhijun, Erwin Emmerling, and Cristina Thieme

In July 1974, the excavation of one of the most spectacular archaeological finds of this century began: the Terra-cotta Army of the Emperor consists of more than seven thousand life-sized clay soldiers, six hundred clay horses, one hundred wooden wagons, and thousands of bronze weapons. Most of the clay soldiers are broken. Thousands of shards in all sizes probably date from as early as 206 B.C.E., after the fall of the Qin dynasty, as a rebel army pillaged the grounds, and then later as the wooden roofs above the passages collapsed (Qu and Cheng et al. 1984).

In addition to the difficulties of excavation, conservation of the existing remnants of paint layers covering the figures at the Museum of the Terra-cotta Army, Lintong, Shaanxi, is one of the main concerns of a collaborative project between the Ministry for Cultural Properties of the Province of Shaanxi and the Bavarian State Conservation Office. The entire army of figures was originally painted in color (Fig. 1). Since the clay fragments dry out after being excavated, remnants of their paint layers are always extremely vulnerable and likely to fall off. To develop suitable methods of conserving these endangered paint layers, excavation work on the figures of the Terra-cotta Army was stopped several years ago.

Figure 1
Clay figure with remnants of the paint layer.

Since June 1991, the restoration ateliers of the Bavarian State Conservation Office have been investigating the paint materials, painting techniques and the state of preservation of the polychromy of the army of clay figures. For conservation techniques to be successful, knowledge and correct judgment of the aging phenomena and the causes of damage are fundamental. The first steps to approaching such questions consist of exact determination of the structure of the paint layers and their state of preservation; and research into the composition of the materials, material properties, and the techniques used to manufacture the clay figures and apply the polychromy. Of special importance is information on how the painting materials withstand extreme changes in climate, as are unavoidable during excavation (Thieme et al. 1993:6–54), when the clay figures are brought from wet burial conditions into dry surrounding air.

Manufacturing Techniques for the Terra-cotta Figures

Most of the clay figures are made of a gray terra-cotta, and some of red terra-cotta. The clay figures consist of separate body parts that can be fitted together. The individual parts—torsos, legs, and arms—are built up out of clay coils; other parts were made with the help of molds—negative forms into which the soft clay was pressed to achieve the desired form. Molds were not used to make all the individual parts but were the basic means of standardizing and accelerating production (Ledderose et al. 1990). All fragments are made of very high-quality clay and have been excellently preserved. The tremendous weight of the clay figures (about 200 kg) causes a considerable problem and requires measures to provide physical support, such as textile fabric that is glued onto the inside of the figures to prevent the glued cracks from opening up again.

Painting Techniques and Materials: Construction of the Paint Layers

The top layer of paint that covers the figures completely has a matte surface today. In general, the paint layers consist of a single or double layer of dark brown ground made of organic materials, and of pigmented layers that vary in number and thickness.

Figure 2
Fragment 003-1991 at 84% RH, maximum length 6.5 cm. Incarnate layer (pit 3 – N0264).

Figure 3
Detail of Fig. 2. On the gray terra-cotta is a double layer of dark brown ground made of organic materials (oriental lacquer tree, *Toxicondendron verniciflua*). The rose-colored pigment layer covering the ground layer has soil materials on the surface.

Ground layers

Chemical analysis of the binding medium shows that the main component of both ground layers is the sap of the oriental lacquer tree, the *Toxicodendron vernicifera*. The dark brown ground clearly reacts differently than other oriental lacquers and develops extreme tension during absorption of moisture. This behavior is very similar to that of a layer of glue or a mixture of glue and gum. The ground, however, also demonstrates chemical resistance to organic solvents that is typical of oriental lacquer. Admixtures such as glue or gum might be present in the lacquer but could not be detected by means of infrared (IR) spectroscopy and gas chromatography mass spectrometry (GCMS).

In color, the ground of all the fragments examined in Munich ranges from brown to dark brown. The double-layered ground is applied in two thin layers (total thickness approximately 0.1 mm) and consists only of the binding medium (Figs. 2, 3). The double-layered ground is extremely sensitive to variations in humidity and loses considerable volume during drying, results of which are visible as drastic craquelure and strong buckling of the flakes thus formed.

The single-layered ground is brown, transparent, and extremely thin. In a dry state, it exhibits microcracks. In contrast to the double-layered ground, the single-layered ground is stable with respect to changes in climate and does not pose any conservation problems. The research methods used were infrared spectroscopy, microhydropyrolysis, and microchemistry (Herm 1991).

Pigmented layers

The colored layers differ in number, thickness, and the mixture of pigments used. So far, the only binding medium detected has been oriental lacquer. This seems an unlikely binding medium to use in the pigmented layers, but it was not possible to determine whether another binding medium was used as well.

The optical and physical characteristics exhibited by the paint layers of the clay figures today are similar to the properties of paint with glue as the binding medium. The assumption that this is not a pure lacquer technique is also based on technical observations of the paint properties. The pigments used are not resistant to lacquer. The flesh-colored paint layers consist primarily of bone white, a pigment that turns brown when bound with oriental lacquer. It is still unknown whether typical Chinese painting techniques were used or whether a technique was used that is unique to the Qin figures. Descriptions of painting layers that exhibit similar behavior and produce similar conservation problems after excavation have not been found in the literature.

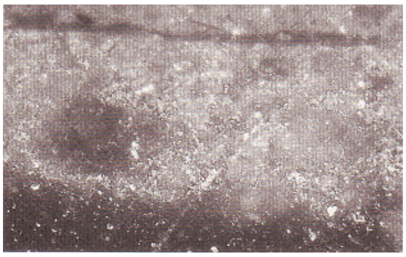

Figure 4
Fragment 003-1992. Cross section of the purple paint layer. Barium copper silicate mixed with cinnabar, ×780.

A typical characteristic of all the flesh-colored paint layers examined is their extreme thickness (0.10–0.20 mm). Identified pigments are bone white, $Ca_5(PO_4)_3OH$, and cinnabar. All examined intact sections of the clay soldiers contain hydroxyapatite, $Ca_5(PO_4)_3OH$. This pigment is manufactured by heating bone to 1000 °C. In contrast to the flesh-colored layers, the red areas are thinly painted. Identified pigments are cinnabar, green, and blue; detected pigments are malachite and azurite. The violet paint is composed of cinnabar and barium copper silicate, $BaCuSi_2O_6$ (Fig. 4). A violet pigment with identical composition was recently detected for the first time by West FitzHugh and Zycherman (1992). The research methods used were X-ray diffractometry (XRD), energy dispersive X-ray fluoresence (EDX), and scanning electron microscopy (SEM-EDX) (Herm 1991).

Damage to the Paint Layers

Visible reactions first occur when the fragments start to dry. The form of damage to the polychrome fragments cannot be generalized. Different kinds of polychromy show clearly differentiated characteristics of paint layers and also different manifestations of damage. These depend on the number of ground layers and the thickness of the colored paint layers, as well as the pigments used.

The most sensitive layer with respect to changes in environment during excavation is the double-layered ground. Loss of water first causes a drastic shrinkage in volume and peeling off from the terra-cotta ("crocodile craquelé"), then the creation of strongly buckled flakes that separate from the terra-cotta substrate (Figs. 5, 6). After drying out, the ground is extremely brittle and breaks very easily. Between the ground and the pigment layers is a recognizable loss of adhesion; movement of the ground causes the pigment layer on top to crack off. After drying, the pigment layer powders when touched lightly.

Conservation Proposal

In the development of a conservation proposal, recognition that the ground was extremely sensitive to humidity was the most important starting point. On one hand, the ground layer must be stabilized against shrinkage during drying; on the other hand, the adhesion and cohesion of the

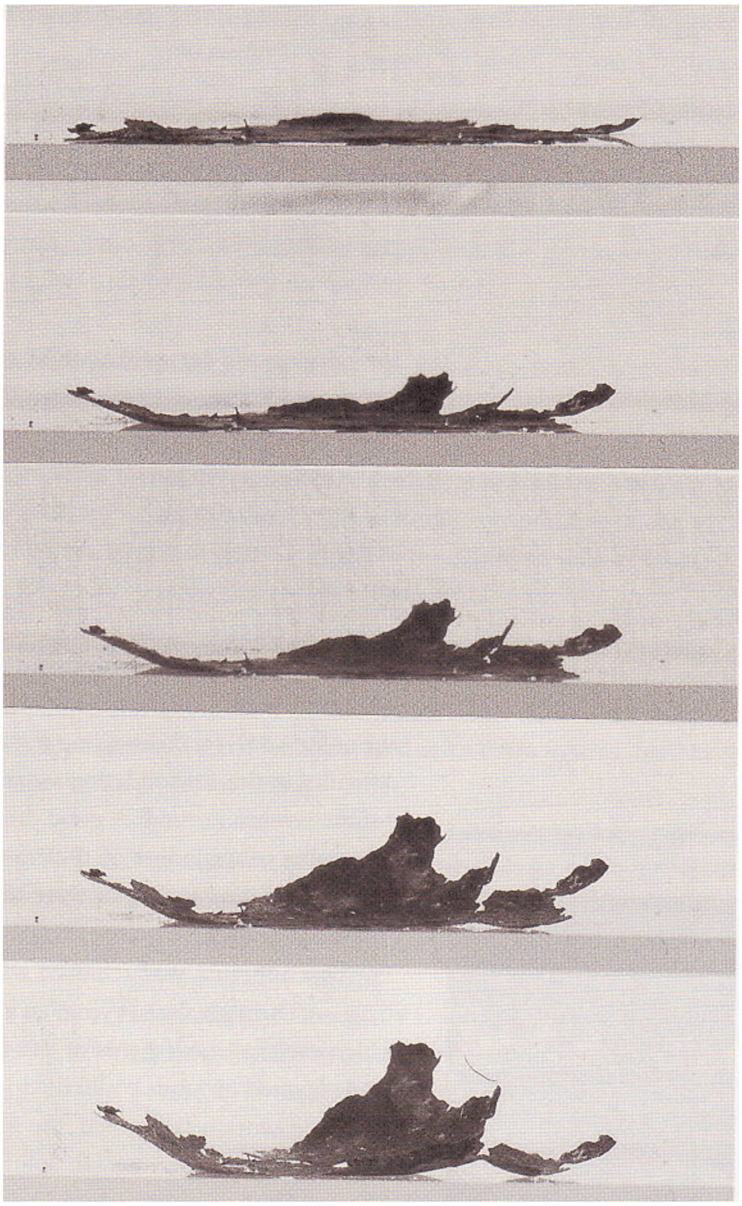

Figure 5
A ground flake (length of the flake when moist: 12 mm) was taken out of the exsiccators with 99% RH and placed in room conditions of about 60% RH. Within four minutes it had buckled considerably, as shown.

Figure 6
Fragment 002-1991 at ca. 60% RH, maximum length 13.5 cm (pit 3 – N0264), showing typical damage to the paint layers.

entire polychromy must be improved or reestablished. Additionally, a technique must be developed to remove the covering of soil from the painted layers in such a way that their original, aged surface is completely preserved. As the basis for the present conservation proposal, the authors formulated the following requirements:

- understanding how the polychromy reacts to slow drying—this will also determine the appropriate point in time for consolidation of the paint layers;
- development of a drying technique;
- stabilization of the ground against shrinkage due to water loss;
- repairing any loss of adhesion between ground and pigment layers;
- repairing any loss of adhesion between ground and terra-cotta substrate;

- repairing any loss of cohesion within the pigmented layers; and
- removal of the soil covering the surface of the paint layers.

Removal of soil from the painted surfaces

Various soil materials adhere to the surfaces of the fragments. Fine-grained, mudlike earth can be removed easily by fine brushes but leaves a residue on the paint surface that makes it appear "yellowed."

Slow drying and determination of the appropriate time for consolidation

Fragments with single-layered grounds can be dried without having to be consolidated beforehand. During the course of slow drying, fragments with double-layered grounds showed a loosening of the paint layers starting at 95% relative humidity (RH), and the polychromy fell off at around 84% RH. Consolidation of the paint layers must be done while the layers are still wet and carried out in humid, saturated air.

Consolidation and demoisturization

The work was done in an enclosed, climate-controlled workbench (at about 99% RH), and the fixing media were applied warm. The greatest difficulty in the consolidation work was the impermeability of the damp, double-layered ground. A good distribution of fixing medium was only achievable on the edges of the craquelure and on the cracks. The following consolidation materials were tested: carboxymethylcellulose, isinglass (fish-bladder glue), Chinese isinglass, Chinese gelatin, and synthetic resins. The best adhesion was achieved with Chinese isinglass.

Through slow drying, an attempt was made to limit the rate at which extreme movements of the ground took place. Paint layers with single-layered grounds could be dried without any problems. After the consolidation work was finished, the first series of experiments in slow drying rates was started. Various salt solutions were studied in exsiccators at different levels of relative humidity (the levels differed in steps of 10% RH). Although the fragments examined in Munich were very small, it took about four weeks to remove the water, regardless of the humidity level. This means that for larger fragments, drying times could run to several months.

For the purpose of developing a method that could be easily implemented on-site, a process of slow drying in boxes of sand was tried. The painted side of the fragment was covered with plastic wrap. The fragment was then placed, painted side down, into a sandbox and covered with slightly moist sand. Under the pressure of the sand, water evaporates slowly out of the ground layer through the terra-cotta. For fragments with a single-layered ground, these methods can be a practical and simple solution (Fig. 7).

Figure 7
Fragment 002-1992. State of preservation after the conservation work at ca. 60% RH.

Freeze-drying

This experiment used freeze-drying to dry and consolidate double ground layers that were saturated with moisture. Normally, freeze-drying is done in two steps: freezing, then drying. As a test material, two flakes of double-layered ground were placed on a substrate of paper and frozen in the freezer compartment of a refrigerator for about twenty minutes at −20 °C. Then the samples were put into the drying unit of a freeze-dryer and cooled to a temperature of about −45 °C (final pressure: 0.04 mbar). The drying process lasted about two hours. The freeze-drying produced the best results thus far in preserving the double-layered ground. Several tests of this process need to be done to optimize the drying conditions.

Next Steps and Questions

Scientific examinations

Further research needs to take place to

- develop appropriate analytical procedures for clear identification of the material composition of the ground and of the binding media in the pigmented layers; and
- investigate the effects of organic additives on oriental lacquer and the aging of the binding media mixtures.

Conservation work

To appropriately conserve excavated terra-cotta figures, further work needs to be done, including

- investigation of other fragments for a more complete understanding of the composition of the paint surface;
- experiments with freeze-drying with the aim of optimizing drying conditions; and
- adaptation of laboratory results to the excavation situation in Lintong for use in on-site restoration workshops and in a proposal for developing a suitable infrastructure for on-site restoration work.

Conclusion

According to today’s state of knowledge, a further excavation of the terra-cotta army would have harmful effects on the colored layers, as the risks connected with the climatic problems during excavation have still not been overcome. Conservation of the polychromy can only be ensured if the excavations are carried out according to the capacity of the equipment and in accordance with all other knowledge of conservation developed during this and any further research.

Acknowledgments

This work has been supported by the Bundesminister für Forschung und Technologie (BMFT), Germany.

References

Herm, C.
1991 Pigment- und Bindemitteluntersuchung der Farbfassung der Terrakottaarmee. *Forschungsberichte des Bayerischen Landesamtes für Denkmalpflege* 8. [1993; 12.1993.]

Ledderose, L., et al.
1990 *Der erste Kaiser von China und seine Terrakottaarmee.* Catalogue of an exhibition at Museum am Ostwall, Dortmund, 12 August–11 November 1990. Gütersloh and Munich: Bertelsmann Lexikon Verlag.

Qu, H. J., Z. U. Cheng, et al.
1984 Excavation reports, Shaanxi. German translation by C. Lin. *Forschungsbericht des Bayerischen Landesamtes für Denkmalpflege* 7.1992.

Thieme, C. et al.
1993 Zur Farbfassung der Terrakottaarmee des I. Kaisers Qin Shihuangdi: Untersuchung und Konservierungskonzept. *Forschungsbericht des Bayerischen Landesamtes für Denkmalpflege* 12.1993, Munich.

West FitzHugh, E., and L. A. Zycherman
1992 A purple barium copper silicate pigment from early China. *Studies in Conservation* 37(3):145–54.